University of Stavanger

FACULTY OF SCIENCE AND TECHNOLOGY

MASTER'S THESIS

Study program/specialization: Material design and construction / M.Sc	Spring semester, 2012 Open
Author: Bjørn Tangvald	…… (signature author)
Thesis Advisor: Charlotte Obhrai - UiS	
Title of Master Thesis: Comparison of offshore wind profiles using FINO-1 and FINO-3 data.	
ECTS: 30	
Subject headings: Comparison of measured and predicted offshore wind profiles, Stability correction of wind profiles, Pena, Tambke, Barthelmie.	Pages: 46…… + attachments/other: 49…… Stavanger, 18.06.2012

Preface

I would like to use this section to thank everyone that has helped me with this thesis both academically and motivationally. First of all I would like to acknowledge and extend my gratitude to my supervisor Dr. Charlotte Obhrai for providing me with FINO data set, Matlab codes, relevant theory and papers, plus giving expellant feedback and help. Thank you very much.

I am grateful to Gunnar Gudmundsen and Sveinung Rasmussen for helping me with Matlab coding when I was lost in a loop. Further must thank my family for all the help with the thesis and academic work throughout the years, and also providing me with a little push when needed.

Finally I would like to thank all my fellow students and UiS for five great years, with lots of fun and learning.

Abstract

The use of wind energy for power purposes has a long history going back to the medieval times. In recent times the wind energy has experienced a great development in both size and the energy output it can produce. Previously use of wind turbines was constricted to land only, but because of the increasing need for reliable and also the wish for cleaner energy, wind turbines are now being placed in offshore environments.

The theories being used to understand the wind forces and conditions are the same as used for onshore applications, however recent research concludes that this assumption is not always correct. One of the areas where this simplification has shown to be incorrect is in the structure of the *atmospheric boundary layer*, and the height of the *surface layer*, which can be problematic since this is the areas where the wind turbines are operating. In order to get a better and more correct understanding of the actual conditions new methods must be derived.

This thesis looks at offshore wind profile that will be appropriate for wind turbines located at sea. The thesis has focused on comparing theoretically calculated wind profiles with actual wind speed measurements (FINO-1 and FINO-3), and further tried to describe and display the accuracy of the different methods. Also a theoretical basis is given to understand the driving forces behind the wind profiles. The methods used here are gathered from relevant standards (DNV and Germanischer Lloyds) and a few more recent methods derived from research, which are supposed to give more accurate description of the offshore wind profiles (Barthelmie 2010, Pena 2008 and Tambke 2005). Due to lack of high resolution data the Barthelmie method could not be calculate. There were also problems recreating the Tambke method as it was described in the paper tambke et al.(2005), no results are therefore given from this method.

The results presented in section 5 clearly show that including stability corrections when calculating the wind profiles, give much better plots and RMSE results. Another parameter that greatly affects the wind profile is the roughness length. Standards normally recommend ranges for this parameter, but often a constant value within this range is chosen when calculating the wind profile. Results show that this parameter varies significantly and that the assumption of a constant value is wrong, the roughness length should therefore be calculated for each case since this gives the best results. The results showed that the Pena method gave most accurate predictions, which was as expected because it accounts for stability corrections and the boundary layer height. The logarithmic method with stability corrections also gave good result, but in stable conditions over corrects giving too high values of wind shear.

Table of content

List of figures

List of tables

Nomenclature

1.1 Symbol Description

B	B is a constant derived from empirical data
C	Bulk-Richardson number
G	Geotropic wind
K_1	Drag coefficient of the wave boundary layer
L	Monin-Obukhov length
c_p	Peak wave velocity
f_c	Coriolis parameter
g	Acceleration of gravity
k	von Karman constant
k_p	Peak wave number
u	Wind speed
u_L	Offset wind speed from G
v_L	Offset wind speed from G
r	parameter ranging from -10 to inf.)
z_B	Wave-boundary layer height
z_i	Planetary boundary layer height
z_0	Roughness length
z_i	Planetary boundary layer height
α	Charnock parameter
ρ_{air}	Density of air
ρ_0	Unperturbed densities
ρ_{water}	Density of water
ϕ_m	function of z/L
φ	Latitude
Ω	Earths angular velocity
ψ_m	Integrated function of ϕ_m

Acronyms

1.2 Acronym	Description
ABL	Atmospheric boundary layer
AS	Atmospheric Stability
DNV	Det Norske VERITAS
GL	Germanischer Lloyd
MBL	Marin boundary layer
ML	Mixed layer
MOST	Monin-Obukhov Similarity Theory
UBL	Upper boundary layer
RL	Residual layer
RMSE	Root mean square error
SBL	Stable boundary layer
SL	Surface layer
WBL	Wave-boundary layer

1. Introduction/Background

Power from wind has developed to become an important energy contributor in today's society and is a crucial producer in many countries. Especially within the European Union the share of power from wind is increasing and represents an important method to obtain their goal for 2020 where 20% of all produced power shall be from renewable energy sources. Traditionally wind turbines have been located on land, but because of the need for locations with stable wind conditions wind turbines are now being placed offshore. Up to now, the same theory has been applied to calculate wind forces onshore and offshore, but offshore experiences with wind turbines have shown unexpected increase in maintenance and decrees in life time suggesting that this assumption is not always correct. Better understanding of the wind profiles over water is therefore needed.

In 2010 the University of Stavanger (UiS) and StormGeo began a research project which aim was to get a better understanding of the conditions offshore. So that a better structural design basis can be obtained for the wind turbines and that the estimation of wind energy can be improved. As part of this project master students are going to check the wind force effects on wind turbine, especially fatigue, and also compare different methods of calculating wind profiles correlated with actual wind measurements from wind platforms. This thesis represents a sub-project of the complex to derive improved methods for calculating wind profiles. It is important to be able to predict correct wind profiles as they directly govern the design loads for wind turbines.

An important parameter in this context is the atmospheric stability in the marine environment which greatly affects the wind profile. Atmospheric stability describes the atmospheres resistance to vertical movement. The atmospheric stability is influenced by several factors such as surface surroundings, local heating, with wind speed and many more. In section 2 a basic presentation of the atmosphere and atmospheric stability is made to give an understanding of what affects the wind and how we can account for this when calculating the wind profile. Unfortunately most of the current standards do not include sufficient parameters to account for these effects for wind profile definitions and instead use simplified profiles

The aim of this thesis is to find out how well the methods predict over all and also in different stability conditions. The methods compared are taken from standards (DNV and GL) and newer methods (Barthelmie, Pena and Tambke) that are supposed to be more accurate. The predicted profiles are then compared to measured wind conditions at FINO-1 and FINO-3. The thesis shows the importance of including stability in the prediction of wind profiles.

2. Atmospheric boundary layer

2.1 Definition

The part of the troposphere that is directly influenced by the presence of the earth's surface, and responds to surface forcings with a timescale of about an hour or less (Stull. 1988). The atmospheric boundary layer (ABL) thickness varies greatly depending on external factors, and ranges from some hundreds of meters to 3 kilometers. Offshore this thickness have been proven to be significantly smaller, measurements from experiments have found it to be as low as 50-60 meters (Stull 1988).

Above the ABL is the free atmosphere (FA) where atmospheric parameters, such as humidity and temperature are no longer affected by the surface environment. Equally the wind speed and direction is no longer affected by surface friction and is now considered geostrophic, which means that the Coriolis force and pressure gradient force governs it (Stull 1988).

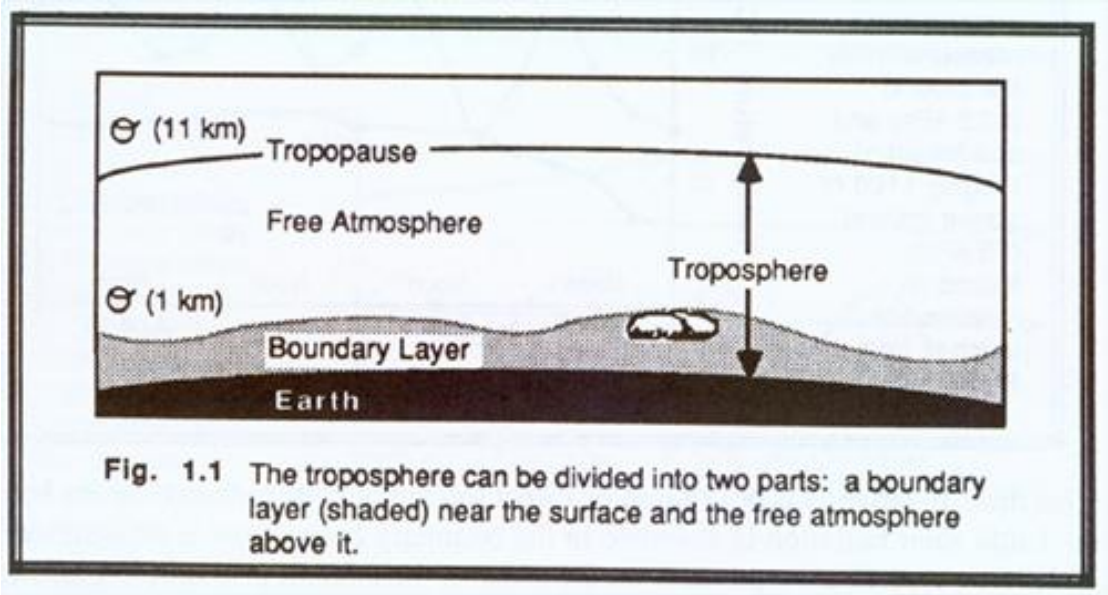

Fig. 1.1 The troposphere can be divided into two parts: a boundary layer (shaded) near the surface and the free atmosphere above it.

Figure 2-1: Shows where the ABL is placed within the troposphere

2.2 The ABL structure

The ABL can be further divided into several sub layers. For a situation over land in a high-pressure region the ABL have a well-defined structure. It is divided in to three main components, i.e. the mixed layer (ML), the residual layer (RL) and the stable boundary layer (SBL). For cases where clouds are present in the mixed layer this layer is further subdivided into a cloud layer (CL) and sub cloud layer (SCL) (Stull 1988). The ABL is influenced by changes in temperature and humidity and evolves with the diurnal cycle (Fig. 2).

Usually the ML develops shortly (half hour) after the sunrise and grows to become the entire ABL during the morning, before it starts to reduce at sunset. Turbulence in the ML is normally characterized as convectively driven, although strong winds are known to form regions with almost well-mixed layers. At dusk the SBL starts to gradually form and will increasing until the ML once again takes over. In contrast to the ML the height of the SBL is not clearly determined but rather has a top that smoothly blends in to the RL above it.

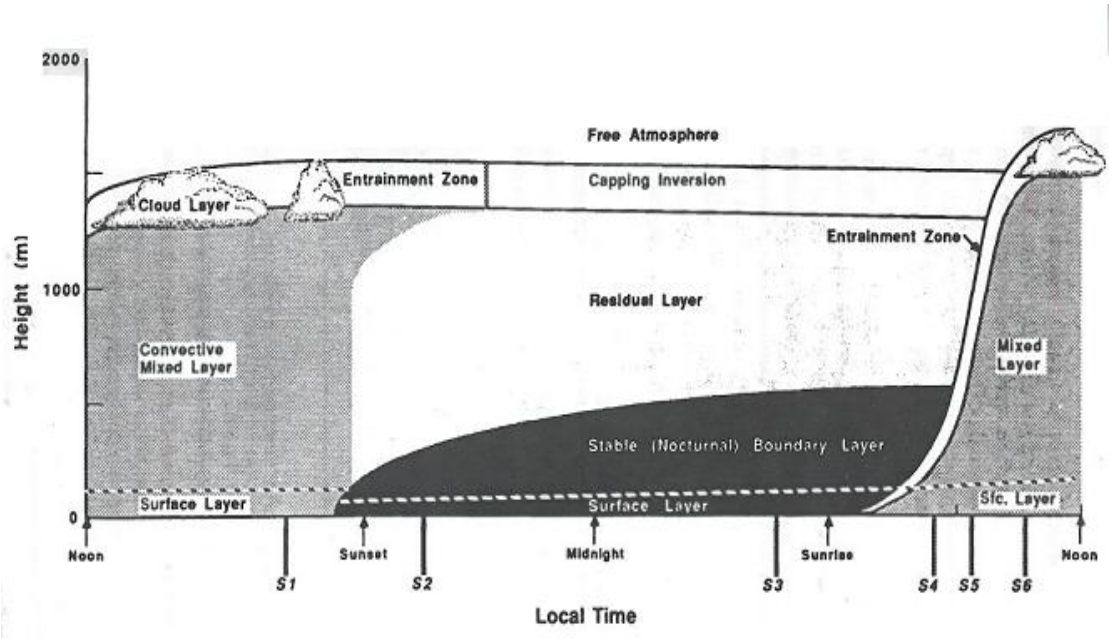

Figure 2-2: The diurnal cycle of the ABL (Stull 1988)

The RL is typically described by natural stratification and isotropic turbulence, whilst the SBL is stably stratified, since the underlying surface is cooling the air. The flow in the SBL is considered laminar (Eugster 2011). Even though the wind at ground level normally settles and calm down at night, strong winds can occur in the interface between the RL and SBL. This is known as nocturnal jet, which enhances wind shear and can generate turbulence. As a result the SBL can experience some of the same conditions as in the ML (Stull 1988).

Offshore no such distinctly diurnal variations exist since the diurnal temperature changes are less pronounced. The energy balance in water is divided over a much larger volume than that of land, and the heat capacity is much greater. This leads to a weaker temperature change in the top layer of water, resulting in a thinner ABL due to the inhabitation of convection to the atmosphere. The offshore ABL therefore tends to be more stable and have less turbulence.

At the bottom of the ABL there is the surface layer (SL) that roughly accounts for 10% of the boundary layer height. In this layer mechanical (shear) generation of turbulence exceeds buoyant consumption or generation. Turbulent fluxes and stresses also stay relatively constant in this layer. Making it possible to assume that the wind speed increases logarithmically with height in neutral conditions, forming the basis for the logarithmic method.

2.3 Atmospheric stability

When trying to describe the profiles of wind and temperature in the ABL it is important to recognize that atmospheric stability (AS) plays an important role. In order to understand how the air flows one regard the air to be a Newtonian, and models it using the Navier-Stokes equation (NS). From the NS equation the turbulence kinetic energy (TKE) theorem is formed, which measure the turbulence intensity and is directly related to the transport of heat, moisture and momentum through the ABL.

The TKE is the mean kinetic energy associated with eddies in turbulent flow, and can be quantified by the mean of the turbulence normal stress. The wind vector $\vec{v}$ with its three components u, v and w is divided in a mean and a turbulent part, making the components have the form $u = \bar{u} + u'$. From the kinetic energy ($E = \frac{1}{2}mv^2$) TKE per unit mass is defined as:

$$TKE = \frac{1}{2}\left(\overline{u'^2} + \overline{v'^2} + \overline{w'^2}\right) \qquad \textbf{2-1}$$

In order to see how the TKE changes with time and influences the atmospheric stability it is further derived in to:

$$\frac{\partial e}{\partial t} = \frac{g}{\theta_v}\left(\overline{\omega'\theta_v'}\right) - \overline{u'w'}\frac{\partial U}{\partial z} - \frac{\partial \overline{w'e}}{\partial z} - \frac{1}{\bar{p}}\frac{\partial \overline{w'p'}}{\partial z} - \varepsilon \qquad \textbf{2-2}$$

I II III IV V VI

The change of TKE with time (I) is here described by a buoyant production/consumption term (II), a shear production/consumption term (III), and the transport of TKE by turbulent eddies (IV), and by pressure perturbations (V), and lastly decay due to dissipation effects (VI) (Stull 1988). If the TKE decreases with time the ABL becomes less turbulent, and likewise more turbulent if it increases.

The TKE budget distinguishes whether the term contributes to production or consumption of kinetic energy. A term can be both a producer and consumer depending on the conditions, i.e. buoyancy and shear, while other do neither but express redistribution vertically.

In atmospheric stability there is a need to distinguish between static stability and dynamic stability, and likewise the relative importance of TKE production from buoyancy and shear. The static stability is reasoned on temperature-based definition of stability. Where the air is statically stable when cold dense air underlies warm less dens air. The opposite applies for statically unstable cases (Stull 1988). A much used method to determining stability is the *lapse rate* concept, which defines the decrease of an atmospheric variable with height, the variable being temperature unless otherwise specified (Glickman. 2000). For a neutral stratified atmosphere the ambient lapse rate will equal that of the dry adiabatic lapse rate, in a non-convective situation, i.e. an air parcel is in balance with its surroundings and experiences no force (Eugster. 2011).

Traditionally the local definition of the lapse rate is taught in classes for static stability. Unfortunately this method has grave shortcomings, and because of this frequently fails in the ML. Instead the *Nonlocal* method or *virtual temperature profile* should be used (Stull. 1988). Where the whole layer is examined rather than just one layer, which is the case in the local lapse rate.

The whole ABL is said to be stable if the virtual temperature $\overline{w'\theta_v'}$ is negative at the surface, or displaced air parcels returns to their starting point. For unstable situations the opposite is true. The ABL is neutral if $d\theta/dz = 0$ or the shear term is much larger then buoyancy (Stull. 1988). The Monin-Obukhov length is the most commonly stability method used today, which resembles the static stability (a description of this method will be given in section 2.4).

While static stability implies the lack of motion or the ability to stay fixed, dynamic stability on the other hand refers to motion. The dynamic stability is driven by the mechanical forces generated by wind shear, and can cause fluids to mix and overturning. This phenomenon is known as Kelvin-Holtz instability, and is the main generator of turbulence in clear air (Woods 1969, Stull 1988). When looking at combined stability of the whole layer on observes that the layer can be statically stable and still dynamically unstable. However, with static instability there must also be dynamic instability.

2.4 Monin-Obukhov length

The Monin-Obukhov length, defined by Alexander S. Obukhov in 1954, describes the effect of buoyancy on turbulent flows, and is applicable for the lower part (10%) of the ABL also known as the surface layer. Physically the Obukhov length (L) is the height where buoyant production of TKE is equal to that of shear. The length is given by:

$$L = \frac{u_*^3 \overline{\theta_v}}{kg\left(\overline{\omega'\theta_v}\right)} \qquad \textbf{2-3}$$

Where u_* is the friction velocity, and $\overline{\theta_v}$ the mean virtual potential temperature, k is the von Karman constant, and g the gravity force, and $\left(\overline{\omega'\theta_v}\right)$ is the mean surface virtual potential temperature flux. The virtual potential temperature flux is given by $\overline{\omega'\theta_v} = \overline{\omega'\theta_v} + 0.61\overline{T}\,\overline{\omega'q'}$. Here θ is the potential temperature, $\overline{T}$ the absolute temperature and q the specific humidity (Obukhov, A.S 1971).

Normally L is negative during the daytime because $\overline{\omega'\theta_v}$ is usually positive then, and positive at night when $\overline{\omega'\theta_v}$ is typically negative. Table 2.1 shows the different stability classes of the Obukhov length. This length is also known as the Monin-Obukhov length because it is an essential part of the similarity theory. Here it is part of the stability parameter, which is defined as $\zeta = z/L$.

Table 2-1: Stability classification for Obukhov length (Venora 2010)

Stability Class	Range
Very stable	0 < L < 200 m
Stable	200 < L <
Near-neutral	|L| > 1000 m
Unstable	-1000 < L < -
|Very unstable	-200 < L < 0 m

2.5 Gradient Richardson number

Another method of determining stability is the *gradient Richardson number*, which can be related to the stability parameter ζ in MOST using the equation 3.13 and 3.14. It is a dimensionless number that expresses the ratio of removal of energy by buoyancy forces due to the production of shear (Turner, J.S. 1979).

The *gradient Richardson number* uses pressure and wind speed to calculate the dimensionless number. It is related to the Monin-Obukhov length by the stability parameter $\zeta = z/L$ and by using this function the Obukhov length can be found.

The gradient Richardson number is given by:

$$R = \frac{g\dfrac{dp_0}{dz}}{p_0\left(\dfrac{dU}{dz}\right)^2} \qquad \textbf{2-4}$$

Where $\frac{dp_0}{dz}$ is the vertical density gradient, $\frac{dU}{dz}$ is the vertical gradient of the horizontal wind speed, g is the gravity force and p_0 the density.

3. Offshore Wind Profiles

The wind profile represents the variations of the mean wind speed with height above the still water level. It is influenced by several factors, among them the roughness length, friction velocity and stability. The most commonly applied profile models are the standard logarithmic and power law wind profiles, recommended in the offshore wind standard (DNV). More recent and further developed methods are being made in the attempt of making even more accurate profiles, below three such methods are described.

3.1 Power law

When calculating the wind speed within the surface layer the logarithmic wind profile has proven to give the most reliable results. But for practical application, this method can be difficult since measurement data as surface roughness and friction velocity are not always available. As an alternative the simple Power law wind profile is often used for engineering purposes or when in situ data are not available. The power law wind profile is a relationship between wind speeds at different heights, with the power law exponent α accounting for stability correction. The wind profile is given by:

$$U(z) = u_{ref}\left(\frac{z}{z_{ref}}\right)^{\alpha} \qquad \textbf{3-1}$$

where u_{ref} is the velocity at a reference height, z_{ref} is the reference height, z is the height and α is the power law exponent . In the GL standard this exponent is set to 0.14 for all wind speeds. This is justified by assuming neutral atmospheric stability and a constant surface roughness length of 0.002m (GL 2005).

3.2 Logarithmic profile

For a neutral situation in the lower part of the ABL where TKE is only produced by wind shear and surface stress, the logarithmic wind profile is valid. In this surface layer the wind speed will increase logarithmically with height of the layer. With the knowledge of a wind speed u at an altitude z, the profile within the SL can be calculated by

$$u(z) = \frac{u_*}{k}\ln\frac{z}{z_0} \qquad \textbf{3-2}$$

Where u_* is the friction velocity, k is the von Karman constant (equal to 0.4) and z_0 is the roughness length. The friction velocity is defined as $u_* = \sqrt{\tau / \rho_a}$, where τ is the surface shear stress and ρ the air density (DNV-RP-C205). If these variables are not known, but the wind speed at a height is, u_* can be found by rearranging the equation for the wind profile.

Wind profiles are greatly affected by the stability in the ABL, and the logarithmic profile is therefore modified to include stability correction. The derivation of the logarithmic wind profile follows the publication of Holtslag (1984)

From Monin-Obukhov similarity theory (MOST) it is assumed that a non-dimensional wind gradient can be written as

3-3

$$\frac{kz}{u_*}\left(\frac{\delta U}{\delta z}\right) = \phi_m\left(\frac{z}{L}\right)$$

where ϕ_m is a function of z/L and U is mean wind speed at height z. There have been proposed several forms of the function ϕ_m for unstable conditions (L<0), but is here set to

$$\phi_m = \left(1 - 16z / L\right)^{-1/4} \qquad \textbf{3-4}$$

For stable conditions (L>0) there is a consensus that ϕ_m should be written as

$$\phi_m = 1 + \alpha \frac{z}{L} \qquad \textbf{3-5}$$

Dyer (1974) proposes that the coefficient α is set to $\alpha = 5$ for moderate stable conditions. There is an ongoing academic discussion whether this coefficient varies with stronger stabilities (Holtslag 1984).

When integrating the *non-dimensional wind gradient* over the height z the wind speed profile is given by:

$$U(z) = \frac{u_*}{k}\left[\ln\left(\frac{z}{z_0}\right) - \psi_m\left(\frac{z}{L}\right)\right] \quad \textbf{3-6}$$

Here the stability correction ψ_m is found by

$$\psi_m\left(\frac{z}{L}\right) = \int_0^{z/L} \frac{1-\phi_m(\zeta)}{\zeta} d\zeta \quad \textbf{3-7}$$

This gives a stability correction ψ_m for unstable conditions like

$$\psi_m = 2\ln\left(\frac{1+x}{2}\right) + \ln\left(\frac{1+x^2}{2}\right) - \tan^{-1}(x) + \frac{\pi}{2} \quad \textbf{3-8}$$

Where $X = (1-19.3\zeta)^{1/4}$, for stable conditions

$$\psi_m = -\alpha\frac{z}{L} \quad \textbf{3-9}$$

3.3 Roughness length

The roughness length z_0 is found through the Charnock relation that ties the roughness together with the surface friction velocity.

$$z_0 = \frac{A_c U_*^2}{g} \quad \textbf{3-10}$$

Where A_c is the Charnock constant and U_* the friction velocity. This method does not explicitly incorporate information on the wave state, but assumes that its influence can be represented by the surface stress. If friction velocity is unknown the roughness length can be found implicitly by rearranging the logarithmic profile equation to make U_* the unknown, z_0 then becomes

$$z_0 = \frac{A_c}{g}\left[\frac{kU(z)}{\ln(z/z_0)}\right]^2 \qquad \textbf{3-11}$$

The value of roughness length is usually in between 0.0001m for open sea and 0.01m for near coastal areas with onshore wind (DNV-RP-C205).

3.4 Logarithmic MOST profile

The DNV-RV-C205 standard provides advice regarding *environmental conditions and loads*. In chapter 2 recommended practices for wind actions are given, where section 2.3 reviews *wind modeling*. From this part it is found that different values are used for the stability correction parameter in the logarithmic profile. According to DNV the stability parameter should be modeled as follows

For unstable situations (ζ<0)

$$\psi_m = 2\ln(1+x)+\ln(1+x^2)-\tan^{-1}(x) \qquad \textbf{3-12}$$
$$X = \phi_m^{-1}$$

and in stable conditions $(\zeta \geq 0)$

$$\psi_m = -\alpha\frac{z}{L} \qquad \textbf{3-13}$$
$$\alpha = 4.8$$

There is also given an empirical relationship between the gradient Richardson number and the Monin-Obukhov length. This relationship have an upper limitation 0.2, values above this are not valid. From section 2.3 in the standard the Monin-Obukhov length L_{MO} is found this way

$$L_{MO} = \frac{z}{R} \qquad \textbf{3-14}$$

unstable conditions

$$L_{MO} = z\frac{1-5R}{R} \qquad \textbf{3-15}$$

stable conditions

3.5 Pena

The logarithmic MOST wind profile (described in section 3.3) is only valid for cases where the height *z* does not exceed the surface layer (SL), over this height deviations will occur. In order to have a method also valid for heights above the SL this method have been further developed to extend from the SL to the entire atmospheric boundary layer

The mean wind shear profile is derived following Gryning et al (2007) like

$$\frac{\partial u}{\partial z} = \frac{u_*}{kl} \qquad \textbf{3-16}$$

Where u is mean wind speed at height z, $u_*$is the friction velocity, k is von Karman constant and *l* is the local length scale. Within the SL that accounts for roughly 10% of the ABL, the wind profile is expressed as in eq. 3.5. Here the stability correction $\psi_m(z/L)$ is based on the relation from Businger et al for stable condition and Grachev et al in unstable condition, when conditions are neutral ψ_m is zero (Pena 2008).

In the ABL above the SL friction velocity decreases with the height as

$$u_* = u_*\left(1-\frac{z}{z_i}\right)^{\alpha} \quad \textbf{3-17}$$

Where z_i is the height of the ABL and α a variable described in Gryning et al (2007), but here put as equal 1. This assumption is only valid for stable and neutral conditions.

The height of ABL is given as.

$$z_i = 0.12\frac{u_*}{f} \quad \textbf{3-18}$$

Where f is the Coriolis parameter given as

$$f = 2\Omega\sin(\varphi) \quad \textbf{3-19}$$

Ω is the rotational velocity of earth, and φ the latitude of the location. The wind profile is extended for the entire ABL, by assuming that the length scale is an inverse summation of the three length scales

$$\frac{1}{l} = \frac{1}{L_{SL}} + \frac{1}{L_{MBL}} + \frac{1}{L_{UBL}} \quad \textbf{3-20}$$

where L_{SL}, L_{MBL} and L_{UBL} are the length of the surface, middle boundary and upper boundary layers, respectively. This can be explained by assuming that wind profile in the entire ABL is a linear sum of wind profiles in the surface, middle boundary and upper boundary layers. The MBL is not proportional to z but varies with the AS, UBL is assumed to be the height of the ABL.

$$l_{UBL} = (z_i - z) \quad \textbf{3-21}$$

Under neutral conditions i.e. when $\phi_m = 1$, eq. 3.17-3.19 are put in to eq. 3.16 resulting in

$$\frac{\partial u}{\partial z} = \frac{u_*}{k}\left(1-\frac{z}{z_i}\right)\left(\frac{1}{z}+\frac{1}{l_{MBL}}+\frac{1}{z_i - z}\right) \quad \textbf{3-22}$$

Integrating the eq. over the height gives

$$u = \frac{u_*}{k}\left[\ln\left(\frac{z}{z_0}\right)+\frac{z}{l_{MBL}}-\frac{z}{z_i}\left(\frac{z}{2l_{MBL}}\right)\right] \quad \textbf{3-23}$$

Neutral condition

In stable and unstable condition the wind profile are as follows

$$u = \frac{u_*}{k}\left[\ln\left(\frac{z}{z_0}\right)-\psi_m\left(\frac{z}{L}\right)\left(1-\frac{z}{2z_i}\right)+\frac{z}{l_{MBL}}-\frac{z}{z_i}\left(\frac{z}{2l_{MBL}}\right)\right] \quad \textbf{3-24}$$

stable condition

$$u = \frac{u_*}{k}\left[\ln\left(\frac{z}{z_0}\right)-\psi_m\left(\frac{z}{L}\right)+\frac{z}{l_{MBL}}-\frac{z}{z_i}\left(\frac{z}{2l_{MBL}}\right)\right] \quad \textbf{3-25}$$

unstable condition

With assuming $z >> z_{MBL}$ the profile can be rewritten as

$$u = \frac{u_*}{k}\left[\ln\left(\frac{z}{z_0}\right)\right] \quad \textbf{3-26}$$

Neutral condition

$$u = \frac{u_*}{k}\left[\ln\left(\frac{z}{z_0}\right)-\psi_m\left(\frac{z}{L}\right)\left(1-\frac{z}{2z_i}\right)\right] \quad \textbf{3-27}$$

stable condition

$$u = \frac{u_*}{k}\left[\ln\left(\frac{z}{z_0}\right) - \psi_m\left(\frac{z}{L}\right)\right] \quad \textbf{3-28}$$

unstable condition

Where the stability parameter ψ_m is set to

$$\psi_m\left(\frac{z}{L}\right) = 2\ln\left(\frac{1+x}{2}\right) + \ln\left(\frac{1+x^2}{2}\right) - \tan^{-1}(x) + \frac{\pi}{2} \quad \textbf{3-29}$$

$$x = \left(1 - 16\left(\frac{z}{L}\right)\right)^{\frac{1}{4}}$$

unstable condition

$$\psi_m\left(\frac{z}{L}\right) = -5\left(\frac{z}{L}\right) \quad \textbf{3-30}$$

stable condition

3.6 Tambke

The Tambke method gives an alternative offshore wind profile that is based on inertial coupling between the Ekman layer of the atmosphere and the currents on the sea. The geostrophic wind is regarded as the driving force for the wind fields located in the lower atmosphere. The momentum is transferred downwards through the Ekman spiral, which is defined by a constant turbulent viscosity. To derive an adequate coupling of the Ekman layer of air and water a third layer is introduced, which is called the wave-boundary layer (WBL). This layer has a logarithmic wind profile that is assumed to reach up to a maximum of 30m.

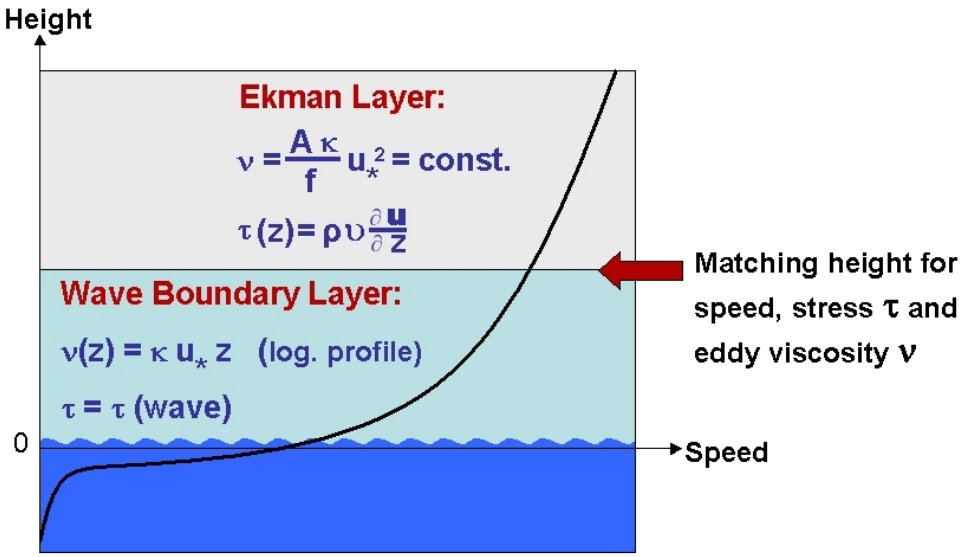

Figure 3-1: Scheme of the vertical wind profile used in the ICWP model (Tambke 2004)

Assumptions made in order to derive the coupling relations:

- *Shear stress is continuous across the interface between air and water*.

  Close to the surface the ratio between the drift velocity of air, u_{air}, and water, u_{water}, is given by the square root of the density ratio of the two fluids. This also applies to the ratio between the friction velocities.

$$\frac{u_{water}}{u_{air}} = \frac{w_*}{u_*} = \sqrt{\frac{\rho_{air}}{\rho_{water}}} \qquad \text{3-31}$$

Where u_* is the friction velocity of the air flow and w_* that of water flow, ρ_{air} and ρ_{water} are the respective densities:

- The layer connecting the two Ekman layers of atmosphere and ocean are assumed to have a constant shear stress. This layer will be denoted as the *wave boundary layer* and extends from a height z_B above to z_B under the water level.
- The turbulent viscosities, ν_{air} and ν_{water} of the two Ekman layers are assumed to be weighted according to the density ratio of the two fluids

$$\frac{\nu_{water}}{\nu_{air}} = \frac{\rho_{air}}{\rho_{water}} \qquad \textbf{3-32}$$

The logarithmic wind profile in the WBL can be described as (Bye 2001)

$$\vec{u}(z) = \left(u_L + \frac{u_*}{k} \ln\left(\frac{z}{z_R} \right), v_L \right) \qquad \textbf{3-33}$$

Valid for $z_R \leq z \leq z_B$

k is the von Karmen constant and z_R is the height where the momentum transfer from the air to the wave field is centered, equivalent to the surface roughness height. The offset (u_L,v_L) is directly given by the geostrophic wind $\vec{G} = (u_g, v_g)$

$$(u_L, v_L) = \frac{1}{2}\vec{G} \qquad \textbf{3-34}$$

The relation that connects friction velocity at the water surface to the geostrophic wind is given by

$$\left|\vec{G}\right| = \frac{\sqrt{r^2+1}}{|r+1|} \frac{u_*}{\sqrt{K_1}} \qquad \textbf{3-35}$$

where K_1 is the drag coefficient of the wave-boundary layer, and r is a constant still to be found. Through oceanographic results it has been shown that the height of the

wave-boundary layer is related to the wave field. From this results it is suggested that z_B is reciprocal to the peak wave number k_p of the wave spectrum. The corresponding peak wave velocity is given by $c_p = \sqrt{g/k_p}$. Assuming that c_p is proportional to the wind speed u(z_B) → $c_p = Bu(z_B)$. From this the height of the wave boundary layer can be written as

$$z_B = \frac{B^2}{8g}\frac{(2r+1)^2}{r^2+1}\left|\vec{G}\right| \qquad \textbf{3-36}$$

B is a constant derived from empirical data (Toba 1973). For $z > z_B$ the wind speed in the Ekman layer is described by the Ekman spiral, the profile above the SL is then written as.

$$u(\hat{z}) = \hat{u}_1\left[\cos(\beta\hat{z}) - \sin(\beta\hat{z})\right]e^{-\beta\hat{z}} + u_g \qquad \textbf{3-37}$$

$\hat{z} = z - z_B$ and $\beta = \sqrt{f/(2\hat{\nu})}$, where *f* is the Coriolis parameter, $\hat{\nu}$ is the turbulent viscosity, $\hat{u}_1 = -0.5u_g/r$ and $\hat{v}_1 - 0.5v_g$. At the interface between the WBL and the Ekman layers ($z = \pm z_B$) the stress tensors and the turbulent viscosity is assumed to be continues and therefore allowing the wind profiles to be matched. At $z = z_B$ the height dependent viscosity of the WBL is

$$\nu(z_B) = ku_* z_B \qquad \textbf{3-38}$$

and the constant viscosity is

$$\hat{\nu} = \frac{2}{f}(r+1)^2 u_*^2 \qquad \textbf{3-39}$$

Equation 3.36 and 3.37 are set equal at $z = z_B$, using eq. 3.34 and 3.35. This allows the parameter r be calculated through iteration.

$$\left|\vec{G}\right|\sqrt{K_1}\left(\frac{B}{4K_1}\right)^2\left(\frac{f}{g}\right)\frac{(2r+1)^2}{(r+1)^3\sqrt{r^2+1}} = 1 \qquad \textbf{3-40}$$

where the parameters K_l=1.5x10^{-3} and B=1.3, these are found from oceanographic measurement (Toba 1973). The Coriolis parameter *f* and gravity-force *g* are known constants for the location, and the geostrophic wind can be chosen to match the input of a given wind speed at a specific height. Coriolis parameter is given by $f = -2\Omega\sin\varphi$, where Ω is the earth's angular velocity and φ is the latitude of the location.

3.7 Barthelmie

The influence of humidity flux method is a further development of the Monin-Obukhov similarity theory. Where sensible heat flux is taken in to account when calculating the stability index (z/L).

The wind speed profile is given by eq. 3.5, described in section 3.3 for the logarithmic wind profile. The stability function varies depending on the stability condition. In stable conditions $\psi_m(z/L)$ is given by (Stull, 1988):

$$\psi_m = -4.7\left(\frac{z}{L}\right) \qquad \textbf{3-41}$$

For stable conditions L is positive, and the stability correction will therefore be positive leading to an increased wind shear. In unstable condition L will be negative and reducing the wind shear. The correction is given by:

$$\psi_m\left(\frac{z}{L}\right) = 2\ln\left(\frac{1+x}{2}\right) + \ln\left(\frac{1+x^2}{2}\right) - \tan^{-1}(x) + \frac{\pi}{2} \qquad \textbf{3-42}$$

$$x = \left(1 - 15\left(\frac{z}{L}\right)\right)^{\frac{1}{4}}$$

When absolute value of L increases (z/L→0) conditions moves towards neutral and $\psi_m(z/L) \rightarrow 0$, thus leaving a progressively more logarithmic wind profile.

The virtual kinematic heat flux $\omega'\theta_v'$, in the equation for *L*, is related to the combined effect of sensible and latent heat fluxes. Using the dimensionless form of L (z/L) and the definition of virtual potential temperature, the equation for the Monin-Obukhov length can be rewritten as:

$$\frac{z}{L} = -\frac{gkz}{u_*^3\theta_v}\overline{\omega'\theta'} - 0.61\frac{gkz}{u_*^3\theta_v}\overline{\omega'q'} \qquad \textbf{3-43}$$

Where the first part accounts for sensible heat fluxes (z/L_T) and next accounts for humidity fluxes (z/L_q). Here $\overline{\omega'\theta'}$ is the kinematic heat flux and $\overline{\omega'q'}$ is the humidity flux.

In later studies it has been suggested that the height of the boundary layer should be included, to account for the deviations from the wind profile based on MOST, at least under stable conditions. Gryning et al. (2007) suggest a modification to wind profile under stable conditions that is the same as in eq. 3.25:

In order to use this method high resolution recording of the wind speed is needed so that the Monin-Obukhov length can be calculated. In this thesis only the 10 min mean wind recordings have been available and it has therefore not been possible to investigate this method. The review of this method has only contained the basics so that a light understanding of the method may be provided.

4. Dataset and instruments

The FINO-1 and FINO-3 wind platforms are sited in the North Sea just outside the coast of Germany and Denmark. They were built as part of the FINO research project, where the objective is to learn more about the offshore conditions at possible wind park sites, and optimization of the offshore wind turbine design.

In order to get a good understanding of the conditions wind turbines experience the wind platforms have to gather information in the same height range as the turbines. Because of this both platforms stretches up to heights over 100 meters. Wind direction, air and water temperature, moister and air pressure are also measured to get a comprehensive picture of the meteorological situation.

At the FINO-1 site the wind tower is design with two booms with measuring equipment on either side as shown in figure 4.2. This leaves a small unmeasured zone, as illustrate in the figure, but still provide more than sufficient data measurements.

4.1 Site description

4.1.1 FINO-1

The FINO-1 platform have been operating since the mid of 2003 and is sited about 45 km off the island of Borkum in the North Sea. A series of cup anemometers on the south-east side are used to measure the long term wind speeds at the heights between 33.5m to 101.5m. While wind directions are found on the north-west side using wind vanes located at several heights (33.5m, 50m, 70m and 90m). High resolution ultrasonic anemometers are installed at intermediate heights (40m, 60m and 80m). These measuring devices are located on one boom to get undisturbed recordings, and cup anemometers are on the other boom.

At the FINO-1 site the wind tower is design with two booms with measuring equipment on either side as shown in figure 4.2. This leaves a small unmeasured zone, as illustrate in the figure, but still provide more than sufficient data measurements.

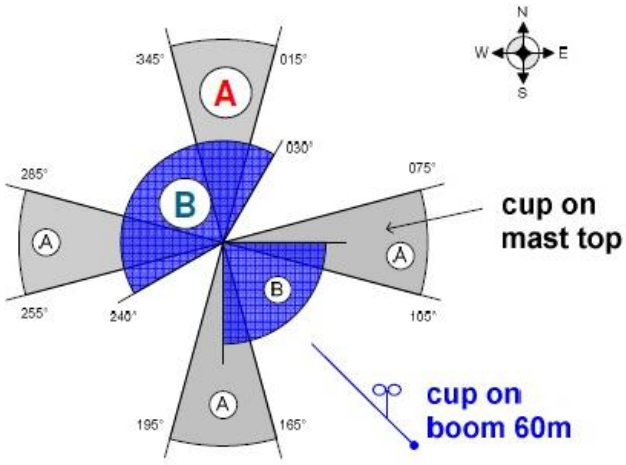

Figure 4-1: Arrangement for measuring equipment on FINO-1

4.1.2 FINO-3

FINO-3 is located 80km west of Sylt in the North Sea of Schleswig-Holstein and has been operating since the end of august 2009. The water depth at the location is 22m, and wind speed measurements are taken at several heights from 30m up to 105m. Complete undisturbed wind speed recordings are found at the intermediate levels (50m, 70m and 90m).

To minimize the effect of distortion on FINO-3 the wind tower have been designed with a triangular base that have three booms. The measuring devices are placed on a beam slightly outside of the boom. By doing this it creates an undisturbed wind sectors of 2 x 60^0 (figure 4), where reliable results can be recorded.

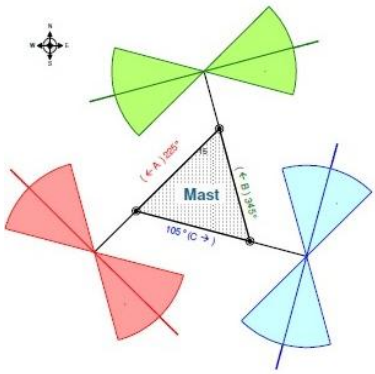

Figure 4-2: Measuring equipment arrangement at FINO-3

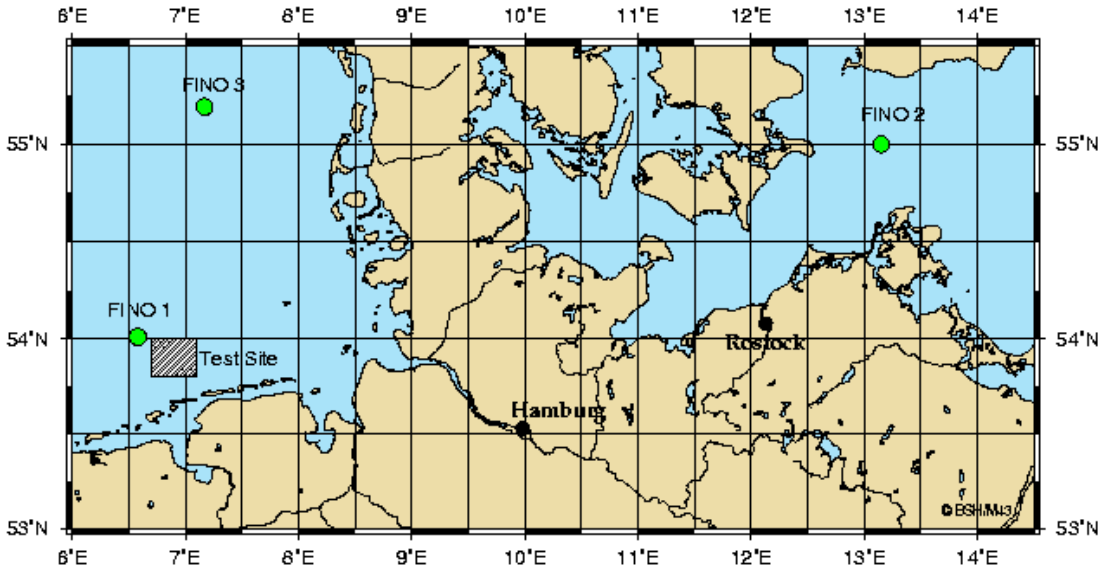

Figure 4-3: Map with grid plot showing where the sites are located

4.2 Data description

4.2.1 FINO-3:

The data set used here extends over a period of two years, stretching from October 2009 to October 2011, with a data return of 77%. This resulted in a data set containing approximately 81,000 records of 10 minute average values. In order to use the data set it was filtered to remove non-stationary conditions, this was done by checking for the following situations:

- That variation in u was less than 10%.
- Temperature *T* varied by less than 0.5 ^{0}C.
- Wind direction changes were less than 10^{0} between consecutive values.

After this filtration the data set was reduced to 69,000 recordings.

The results from Obhrai (2012) analysis of the data set shows that vary unstable conditions dominate the FINO-3 site (48.6%). This was found using the gradient Richardson number. It was not possible to verify these findings through other methods, such as Bulk Richardson number, because of lack of sea surface temperature measurement due to equipment failure.

4.2.2 FINO-1:

From the FINO-1 site the data used in this thesis was recorded over a two year period from Jan 2006 to Jan 2008, with a data return of 59% in this period. This gave a total of 61.804 10-minute recordings, where 14.14% of the recordings were filtered away because of non-stationary conditions, which reduced the data set used to 53,065. The filter used to remove the non-stationary data is the same as described in section 4.2.1. *Data description FINO-3*.

5. Analysis and results

In this section the analysis and results for each of the different methods are presented for the two different locations (FINO 1 & FINO 3). In accordance with the theory all non-stationary conditions were removed, which reduced the data set by approximately 14.4% and 14.8% for FINO-1 and FINO-3 respectively. The filters applied to obtain this stationary condition are described in section 4.2 regarding the data description. The MO theory used here is only valid within the SL, which is assumed to be approximately the lower 10% of the ABL. In order to comply completely with the theory an additionally filter should be implemented as well, where data with SL height lower than the relevant ratio height are removed (Venora. 2009). This filter has not been implemented in this study because it would lead to the removal of most of the stable conditions, which we are particularly interested in because of its impact on wind turbine fatigue.

5.1 Atmospheric stability

The stability at the two sites are found using the gradient Richardson number and MOST, described in the section 2.5. The MOSTs stability parameter (ζ) is calculated using the Monin-Obukhov length, which can be found using the gradient Richardson number. This relationship is described in the DNV code RP-C205 but has also been used in all the other methods and throughout the stability analysis of the data. As described in section 3.3 the relationship between the L_{MO} and Ri_{grad} number is valid for all negative values of Ri_{grad}, i.e. in unstable condition. For positive values, i.e. stable conditions, this relationship is only valid for values of Ri_{grad} up to 0.2. Values above this limit are therefore not included in our analysis.

Table 5-1: Stability classification of z/L (Barthelmie 2010)

Stability class	Range
Very stable	0.05<z/L<1
Stable	0.01<z/L<0.05
Near-neutral	|z/L|<0.01
Unstable	-0.05<z/L<-0.01
Very unstable	-1<z/L-0.05

The gradient Richardson number is calculated using the temperature readings at (29m and 95m) and wind speed records at (50m and 90m) for the FINO-3 site, while the FINO-1 site use temperature readings at (30m & 100m) and wind speed at (40m

& 80m). These elevations were chosen because they have available measurements for all wind directions. At both sites very unstable conditions were dominate (41.2% and 48.6%), where the FINO-3 had slightly more unstable conditions than FINO-1, which one can see in figure 9.1 in the appendix (Obhrai et al 2012).

5.2 Offshore wind profiles

The results when applying the different wind profile methods are presented in the subsections below. The results are presented in the same manner for all methods, The reasons that one has chosen these ratios are the availability of the measured data and also because these are typical heights for offshore wind turbines, making it an important area to study.

5.2.1 Logarithmic and power law

The results here show the wind speed ratios at 70m/50m and 90m/50m respectively, and are represented as a function of the stability parameter (z/L) where z is equal to 70m an 90m respectively. In figure 5.1 measured wind speed ratio is plotted as scattered red dots, and the mean wind speed is represented as blue dots. This mean value is taken as the average of each stability bin. The horizontal lines crossing the figure are the estimated wind speed ratios calculated using different methods, where the blue line is the power law method and the green and yellow is the logarithmic method with different roughness length. These methods are described in section 3.4 and 3.3 respectively with eq. 3.15 and 3.1 being used to calculate the profile.

The reason for the logarithmic profile being represented twice is because the DNV-RP-C205 standard does not give a clear recommendation of z_0, but rather a range that the roughness lengths. In figure 5.1 the two z_0 represents the expected upper and lower value of this range, with the upper z_0=0.01 and lower z_0=0.0001.

From the figure one can see that neither method gives a good estimate of the wind speed profile and because of the lack of stability correction in methods it ends up predicting a constant wind shear for all stability conditions. The only reasonable estimate is given by the logarithmic method with z_0=0.0001 for the 70m/50m ratio in the unstable zone, where the plots are relatively consistent. From figure 5.1 and 5.2 one can see that the methods over predict the shear and also that the ratio gets more correct with z_0=0.0001. This agrees well with results establish when calculating the roughness length using the Charnock relation, where it was found to be in the range of 1e-3 to 1e-5. These results are not surprising as none of the methods include stability correction, and are therefore according to the theory are not suited to estimate wind speed profiles other than that in neutral and near neutral conditions. It is important to note that also in neutral and near neutral conditions the methods under predicts wind shear.

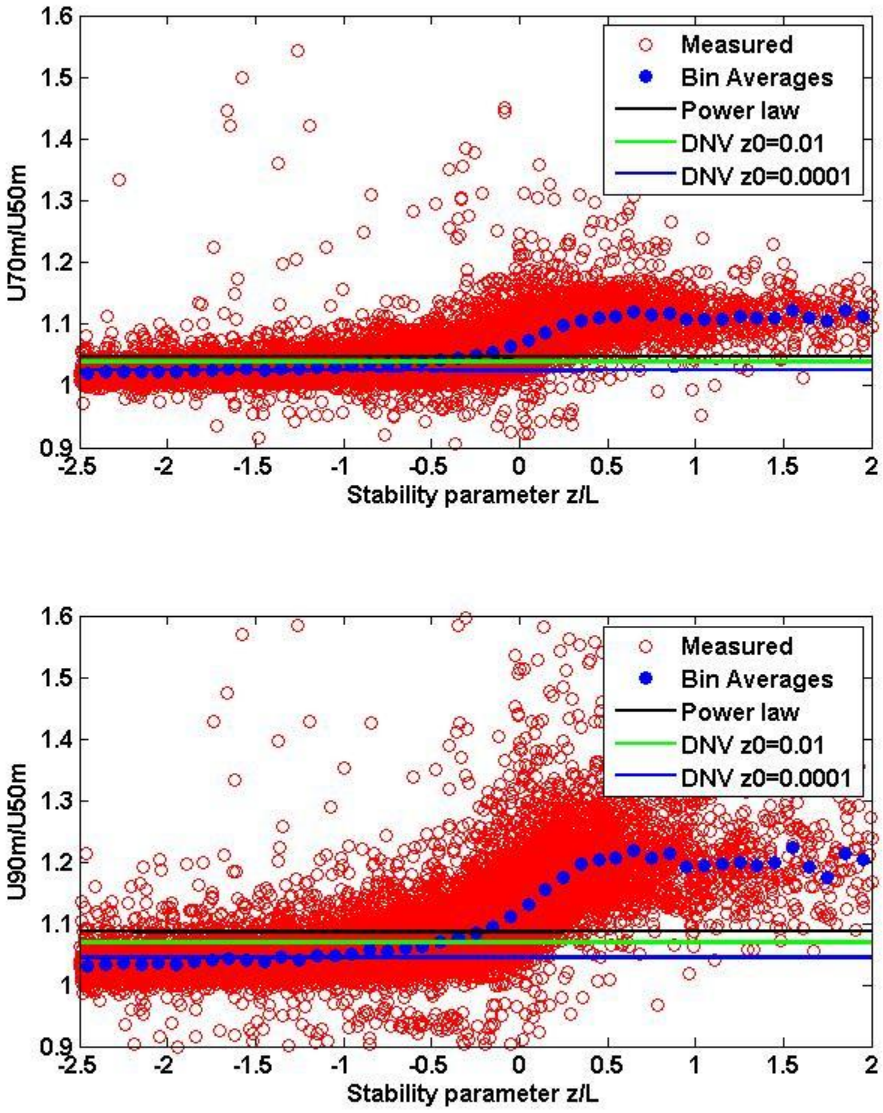

Figure 5-1 Logarithmic and power law method results for FINO-3 at 70m/50m on top and 90m/50m on bottom.

The results and plots from the FINO-1 are presented in the same way as for the FINO-3. In figure 5.2 one can see that neither method gives good estimates of the wind profile ratio, but in unstable condition the ratios are closer than in stable condition. Also for the logarithmic method at 80m/40m the velocity ratios have a much closer ratio, meaning that the roughness length is less dominating.

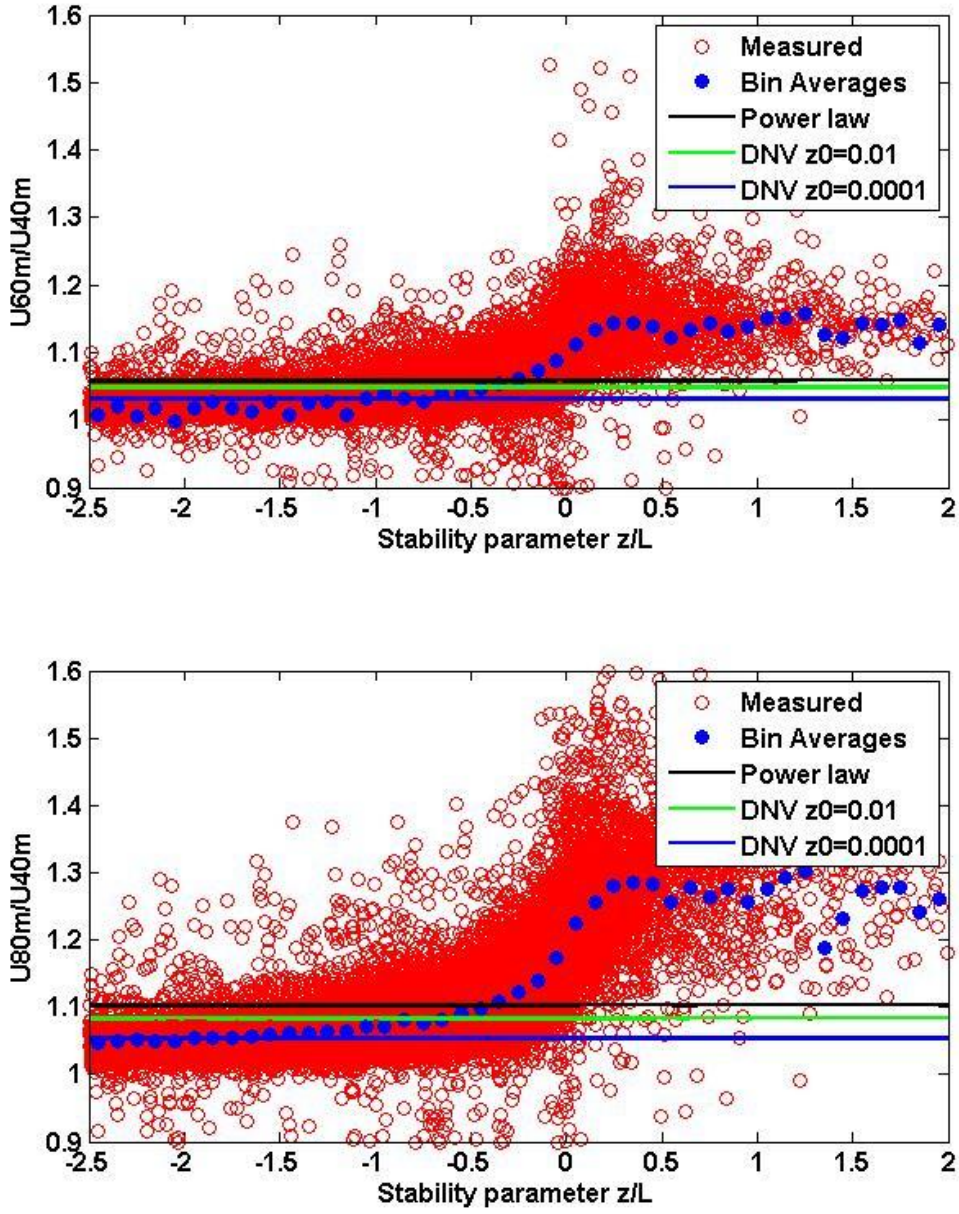

Figure 5-2 Logarithmic and power law method results for FINO-1 at 60m/40m on top and 80m/40m on bottom.

The results from FINO-3 and FINO-1 are fairly similar with both methods showing that they are inadequate to give a good estimate of wind shear outside of the neutral condition. Our results also show that the power law is less reliable method than the logarithmic profile.

5.2.2 Logarithmic with stability correction

The results from the logarithmic profile with stability correction are presented in the same manner as the other logarithmic profile method described in the previous section. Where wind speed ratios at 70m/50m and 90m/50m respectively at FINO-3, are represented as a function of the stability parameter (z/L). The predicted velocity ratio using the logarithmic profile with stability correction is represented with black, green and yellow lines in the figure 5.2, where the difference in the plotted lines are the surface roughness. Two of the plotted lines (green and yellow) use the lower and upper z_0 respectively, while the black one has a varying z_0 that is calculated from the Charnock relation (eq. 3.10 in section 3.2). The logarithmic wind profile with stability correction is calculated using eq. 3.5 (section 3.1). With the stability parameter given in eq. 3.11 and 3.12 (section 3.3), for unstable and stable conditions respectively.

In figure 5.3 we can see that the predicted wind shear using logarithmic profile with stability correction follow more closely the measured data average bin value. The method gives a reasonable estimate of the ratio in unstable condition, but when coming in to the near neutral zone predicted plot starts to deviate from the measured and the ratio increases. This may be explained by the fact that the stability corrections are included within the near neutral and neutral zone. In stable conditions the predicted ratio start to follow the bin numbers, but the predicted ratio increases more than the average bin values and shows that it over-predicts when coming far enough in to the stable zone, (z/L=0.5-1.0). This is more prominent for the 90m/50m ratio then in 70m/50m ratio.

The effect of roughness length on the MOST plots is clearly seen in the figure 5.3, with z_0=0.01 increasing the wind speed ratio and z_0=0.0001 lowering the ratio. As shown in the figure varying roughness length is plotted over and partly under z_0=0.0001, indicating that z_0 is located in the lowest part of the range.

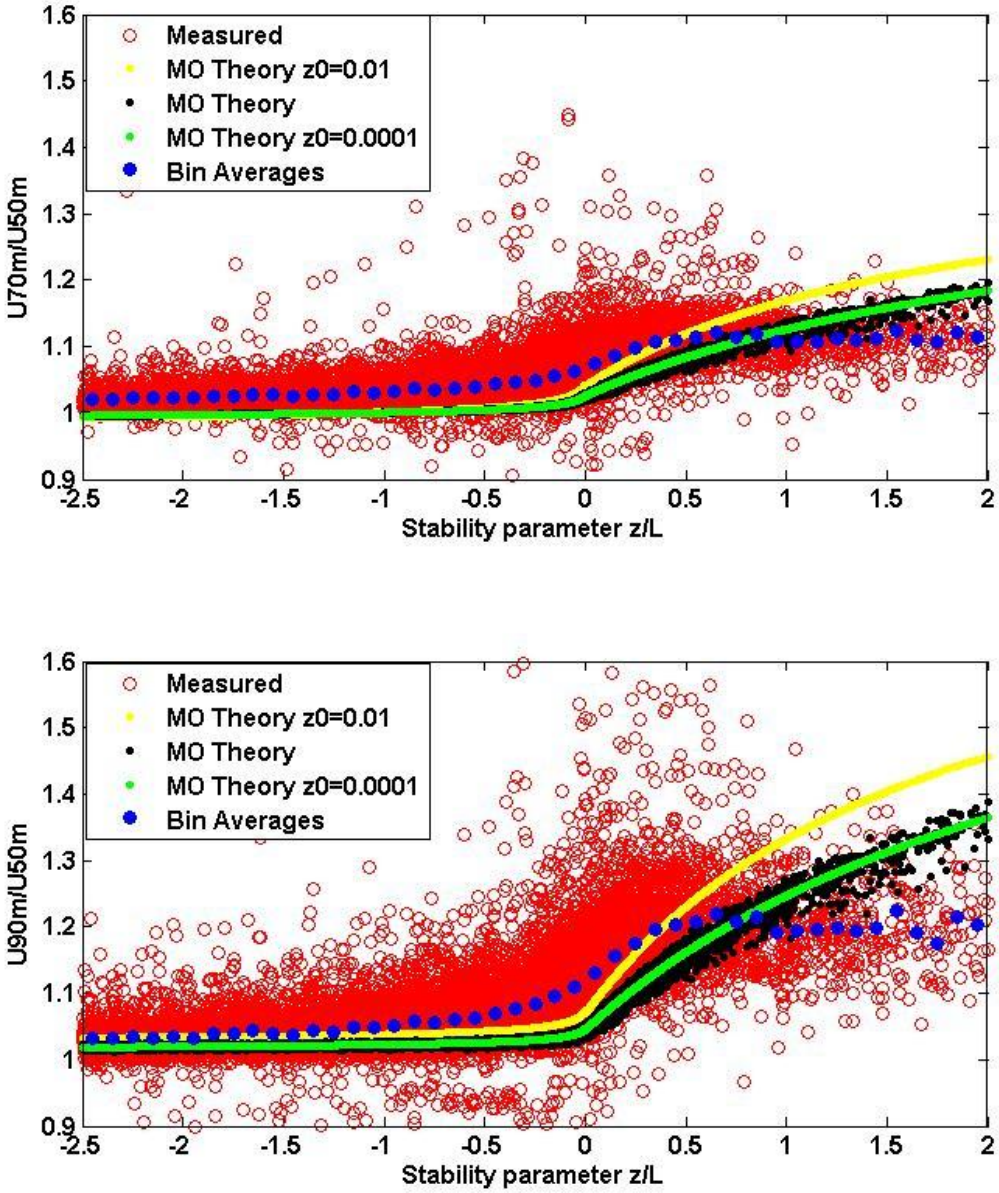

Figure 5-3 MOST profile for FINO-3 at 70m/50 on top and 90m/50m on bottom

The results and plots from FINO-1 are presented in the same way as for the FINO-3 results. Where the logarithmic MOST wind speed ratio is plotted in figure 5.4 for 60m/40m and 80m/40m and more or less show the same results as FINO-3 figure 5.3.

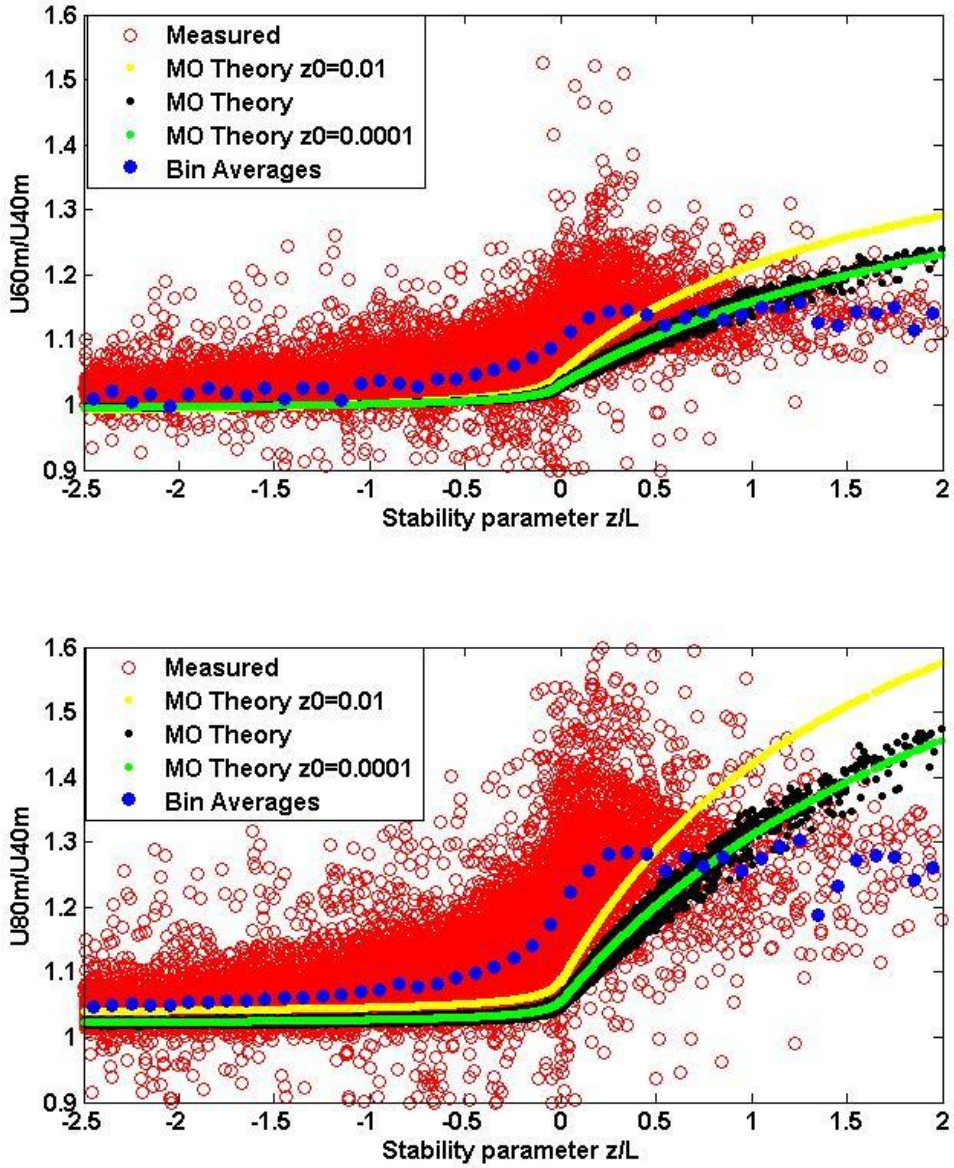

Figure 5-4 MOST profile for FINO-1 at 60m/40 on top and 80m/40m on bottom

Overall the results from FINO-3 and FINO-1 are very similar, with both figures showing the same tendencies. With the only noticeable differences being that the measured values for FINO-1 have an all over higher ratio especially in the neutral zone, and that the calculated values of the logarithmic MOST ratio is higher than FINO-3 in stable conditions.

5.2.3 Pena

The results from Pena are presented in figure 5.5 and 5.6, where the estimated wind ratio is marked as black dots. The wind speed has been calculated from the Pena method described in section 3.5 using equations 3.24-3.26, with stability parameter calculated by eq. 3.27 and 3.28. This method is a further development of the Monin-Obukhov theory where correction for ABL height is added in stable conditions, which is supposed to reduce the wind shear. As described in section 2.1 and 2.2 the ABL height can vary quite much depending on the condition, and in very stable conditions be as low as 50-60m. This method is only valid within the ABL and in cases where ABL height is lower the method can give deviations. Also in section 3.5 eq. 3.34-3.36 were derived by assuming that the MBL height was much lower than the height investigated. This will not be the case in most of the conditions, but because a method to calculate the MBL height is unknown this is disregarded and the eq. used.

In figure 5.5 we can see that the predicted wind ratio follows the measured bin values quite good, but with relatively more scattered than the logarithmic MOST method. The effect of ABL height is clearly seen from the plot, with the Pena plot lying much lower and closer to the average bin values than the MOST profile. For very stable conditions in the 90m/50m plot the scatter becomes quite big, it therefore gets difficult to draw a conclusion on whether the correction for ABL height has any effect. The scatter in the Pena method is also affected by the amount of scatter in the measured values, which one observes when comparing the two heights.

The results from FINO-1 are generally the same as that at FINO-3. With a clear effect of ABL height correction observed. The plot at 60m/40m is more uniform than that at 80m/40m, but this is related to the height ratio being larger. The situation of scattered plots in very stable conditions is more prominent at FINO-1 than in FINO-3.

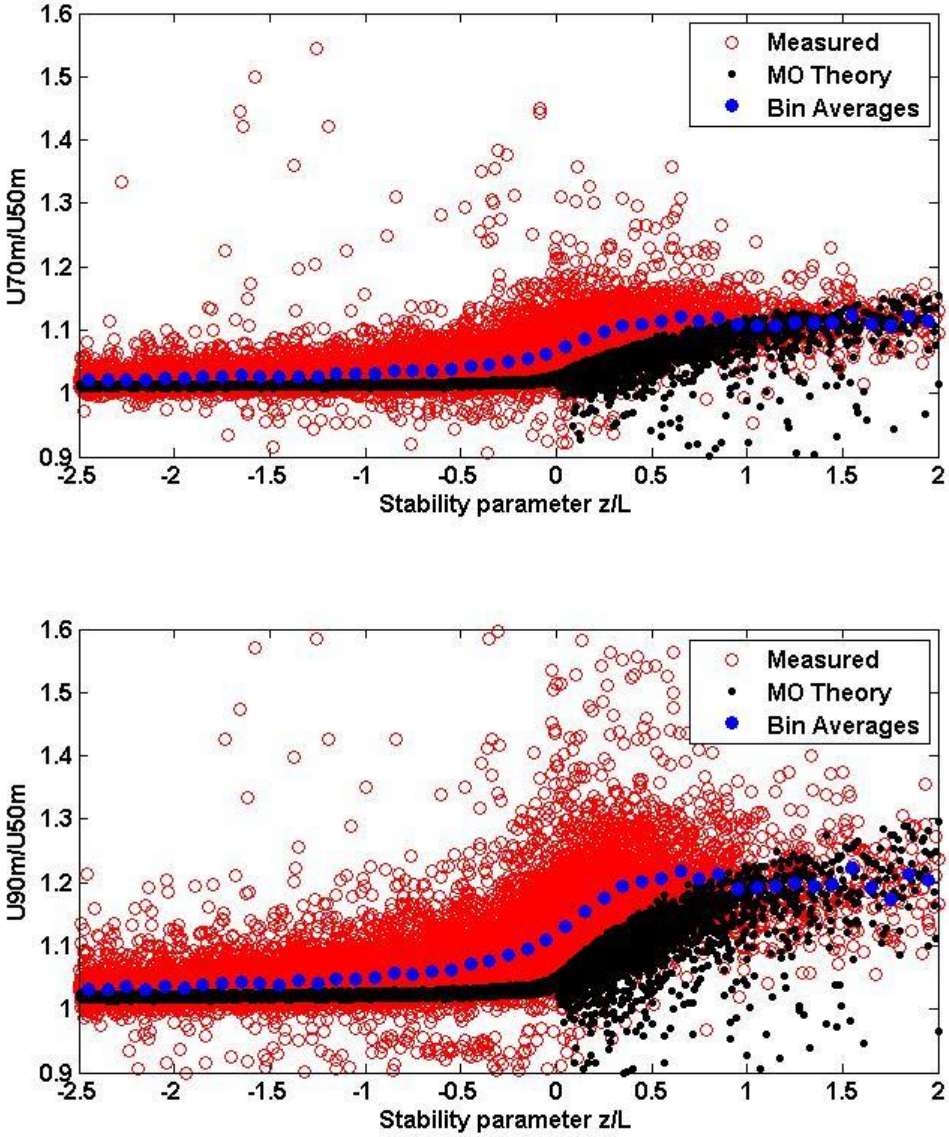

5-5: Pena profile for FINO-3 at 70m/50 on top and 90m/50m on bottom

Overall the figures from both sites show the same tendencies, where the effect of ABL height correction reduces the wind shear and thereby giving a more accurate result. In very stable condition it is unclear whether the ABL height is getting lower than heights being investigated and the theory may therefore start to become invalid.

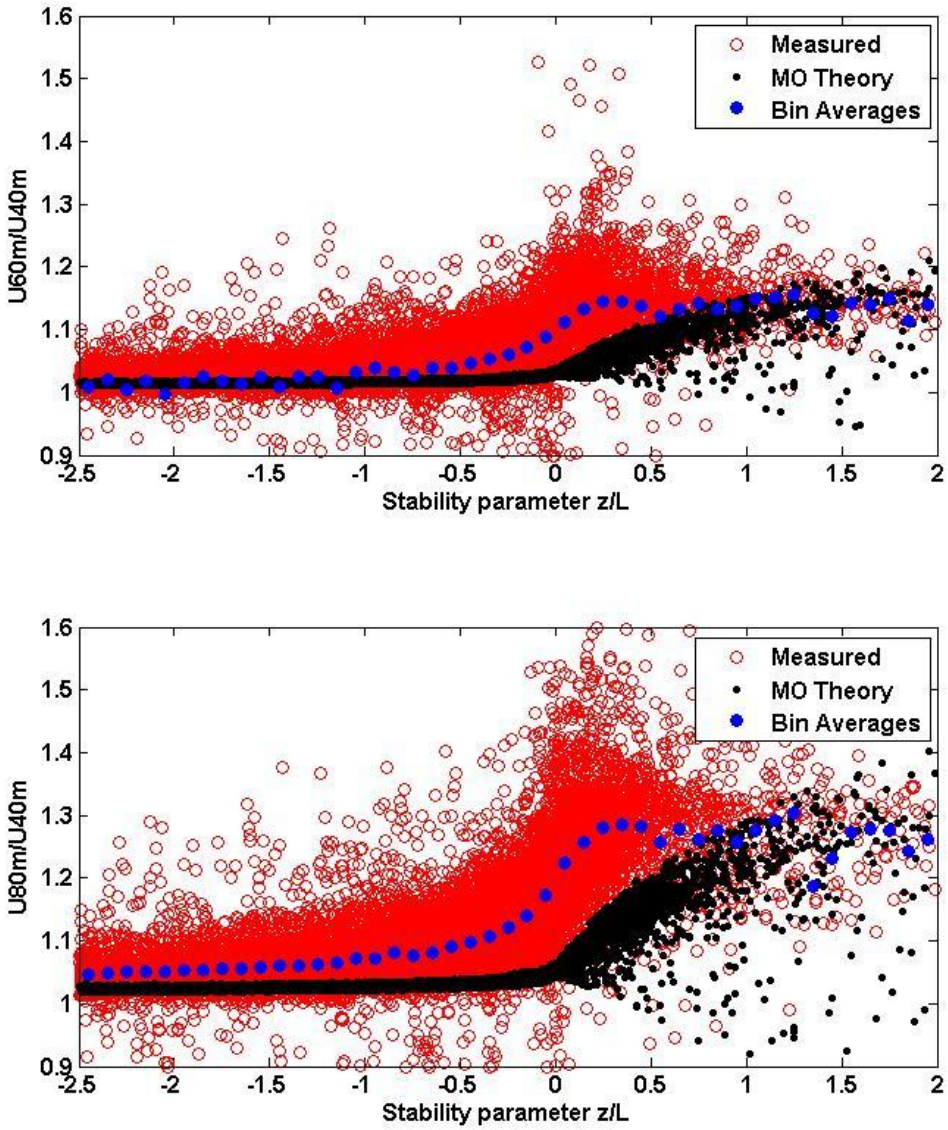

5-6: Pena profile for FINO-1 at 60m/40 on top and 80m/40m on bottom

5.2.4 Tambke

No results are presented for this method because it was not possible to get realistic result by recreate the method as described in Tambke et al. (2005). The problem encountered when recreating the method was how to get a value for the geostrophic wind by only applying a know wind speed. In the paper no suggestion on how to find this parameter is given, which is said to be the driving force of the wind profile, and therefore it is unknown how to calculate the wind profile using this method. A suggestion that have not been tried out is to find the geostrophic wind by iteration using eq. 3.37 and 3.40. A value of G would then be assumed and r would be calculated from eq. 3-40, r would then be used in eq. 3.37 to calculate the wind speed. The predicted wind speed would then be compared to the measured wind speed. If the wind speed do not match the a new value of G is chosen and the steps repeated.

5.3 Comparison of wind speeds

When assessing results it is important to know how reliable they are, and what kind of velocity ratio there are between the predicted and measured values. The velocity ratios are divided into stability classes so that the variations within the data set are better described. Classification of the different stability classes are done according to the stability boundary conditions for the stability parameter given in table 5.1.

Another important method of describing the accuracy of the results is the root mean squared error (RMSE), where the error between predicted and measured wind speed is calculated. The tables bellow summarizes the velocity ratio of measured versus predicted and errors of the different methods used in this study.

The velocity ratio of measured versus predicted and RMSE are calculated using predicted wind speeds at 70m and 90m from FINO-3, and 60m and 80m from FINO-1. The wind speed predictions are made using four approaches:

1. Logarithmic: where eq. 3.2 is used to calculate the wind speed (section 3.2).
2. Power law: uses eq. 3.1 to calculate the wind speed (section 3.1)
3. Logarithmic MOST: where eq. 3.6 is used to calculate the wind speed, stability parameters eq. 3.12-3.13 (section 3.4).
4. Pena: where eq. 3.26-2.28 is used to calculate the wind speed, and stability parameters are calculated from eq. 3.29-3.30 (section 3.5)

In table 5.2-5.5 the mean ratio of all stability classes are presented, where it describes how much the method over or under predict over all. This parameter can give good descriptions of the methods predicting abilities as long as it only over or under predicts. If the method over and under predict depending on which stability condition it is in, the over and under prediction will cancel each other out and the result of the mean ratio will false. Due to this the mean ratio is not used to describe the accuracy of the method.

Table 5-2: Ratio values of the different methods and errors from FINO-3 at 70m

		Stable	Slightly stable	Neutral	Slightly unstable	Unstable	Mean of all data	RMSE
z/L		0.05 < z/L < 1	0.01 < z/L < 0.05	|z/L| < 0.01	-0.01 < z/L < -0.05	-1 < z/L < -0.05		
Ratio predicted/observed wind speed at 70m height								
1. Logarithmic	z0=0.01	1.020	1.024	1.022	1.023	1.017	1.021	0.34
	z0=1e-4	1.007	1.010	1.008	1.009	1.004	1.008	0.28
	z0=varying							
2. Power law		1.029	1.032	1.030	1.032	1.026	1.030	0.40
3. Stability	z0=0.01	1.050	1.027	1.023	1.020	0.995	1.023	0.39
	z0=1e-4	1.028	1.012	1.008	1.007	0.989	1.009	0.32
	z0=varying	1.026	1.012	1.008	1.006	0.989	1.008	0.31
4. Pena		1.021	1.012	1.009	1.006	0.996	1.009	0.31

Table 5-3: Ratio values of the different methods and errors from FINO-3 at 90m

		Stable	Slightly stable	Neutral	Slightly unstable	Unstable	Mean of all data	RMSE
z/L		0.05 < z/L < 1	0.01 < z/L < 0.05	|z/L| < 0.01	-0.01 < z/L < -0.05	-1 < z/L < -0.05		
Ratio predicted/observed wind speed at 90m height								
1. Logarithmic	z0=0.01	1.050	1.054	1.053	1.052	1.040	1.050	0.66
	z0=1e-4	1.026	1.030	1.029	1.028	1.016	1.026	0.52
	z0=varying							
2. Power law		1.066	1.070	1.069	1.069	1.056	1.066	0.79
3. Stability	z0=0.01	1.110	1.060	1.053	1.051	1.028	1.060	0.78
	z0=1e-4	1.068	1.034	1.028	1.026	1.009	1.033	0.61
	z0=varying	1.067	1.033	1.028	1.025	1.003	1.031	0.59
4. Pena		1.052	1.032	1.029	1.023	1.002	1.028	0.60

Table 5-4: Ratio values of the different methods and errors from FINO-1 at 60m

		Stable	Slightly stable	Neutral	Slightly unstable	Unstable	Mean of all data	RMSE
z/L		0.05 < z/L < 1	0.01 < z/L < 0.05	|z/L| < 0.01	-0.01 < z/L < -0.05	-1 < z/L < -0.05		
Ratio predicted/observed wind speed at 60m height								
1. Logarithmic	z0=0.01	1.010	1.020	1.023	1.021	1.011	1.017	0.79
	z0=1e-4	0.993	1.003	1.006	1.004	0.994	1.000	0.85
	z0=varying							
2. Power law		1.019	1.029	1.032	1.030	1.020	1.026	0.54
3. Stability	z0=0.01	1.045	1.024	1.024	1.018	0.985	1.019	0.80
	z0=1e-4	1.017	1.005	1.006	1.001	0.977	1.001	0.82
	z0=varying	1.018	1.030	1.028	1.023	0.977	1.015	0.83
4. Pena		1.014	1.003	1.007	0.999	0.985	1.002	0.50

Table 5-5: Ratio values of the different methods and errors from FINO-1 at 80m

		Stable	Slightly stable	Neutral	Slightly unstable	Unstable	Mean of all data	RMSE
z/L		0.05 < z/L < 1	0.01 < z/L < 0.05	|z/L| < 0.01	-0.01 < z/L < -0.05	-1 < z/L < -0.05		
Ratio predicted/observed wind speed at 80m height								
1. Logarithmic	z0=0.01	1.021	1.035	1.039	1.039	1.026	1.032	0.81
	z0=1e-4	0.993	1.006	1.010	1.011	0.998	1.004	0.77
	z0=varying							
2. Power law		1.177	1.162	1.158	1.157	1.172	1.165	0.90
3. Stability	z0=0.01	1.114	1.061	1.058	1.054	1.023	1.062	0.94
	z0=1e-4	1.063	1.030	1.028	1.024	1.000	1.028	0.82
	z0=varying	1.064	1.030	1.028	1.023	0.997	1.028	0.81
4. Pena		1.034	1.006	1.013	1.003	0.983	1.008	0.83

5.3.1 Logarithmic

In table 5.2 and 5.3 the results from the logarithmic method, relating the velocity ratio between predicted and measured at 70m and 90m respectively at FINO-3, clearly describe that the wind shear is over predicted at both heights when using this method. The method has been calculated using two roughness lengths in according with DNV-RP-C205. From the tables one can see that the method using z_0=0.0001 gives the lowest velocity ratio. The over-prediction is highest in slightly stable conditions and lowest in unstable conditions for wind speeds at 70m. For the logarithmic profile using z_0=0.01 the highest ratio is 1.024 and the min ratio is 1.017. The logarithmic profile using z_0=0.0001 the highest 1.010 and the lowest ratio is 1.004. The same tendencies are seen in table 5.3 for wind speeds at 90m, but with over predictions being higher. As in tab. 5.2 the over prediction here is highest in slightly stable conditions and lowest in unstable conditions. For the logarithmic profile using z_0=0.01 the highest ratio is 1.054 and the min ratio is 1.040. The logarithmic profile using z_0=0.0001 the highest ratio is 1.030 and the lowest ratio is 1.026

The result from FINO-1, given in table 5.4 and 5.5, shows that wind shear generally is over predicted at both heights. This over prediction is highest for both cases in neutral/slightly unstable conditions and lowest for stable conditions, where it actually under predicts wind shear for wind speeds using z_0=0.0001. This may be explained by the fact that this method does not include stability correction which would increase the predicted wind speed. At 60m the profile using z_0=0.01 the highest ratio is 1.023 and the min ratio is 1.010. The logarithmic profile using z_0=0.0001 the highest ratio is 1.006 and the lowest ratio is 0.993. For wind speeds at 80m the profile using z_0=0.01 the highest ratio is 1.039 and the min ratio is 1.021. The logarithmic profile using z_0=0.0001 the highest ratio is 1.011 and the lowest ratio is 0.993.

5.3.2 Power law

The results from the power law method is presented in table 5.2-5.5 where results from FINO-3 are given in table 5.2 and 5.3 while table 5.4 and 5.5 present the results from FINO-1. At both FINO-3 and FINO-1 wind shear is over predicted and increases with height. At FINO-3 the over prediction is highest in slightly stable conditions and lowest in unstable conditions. At 70m the max ratio is 1.0323 and min is 1.0257, with an average of 1.0298. For wind speeds at 90m the max ratio is 1.0703 and min ratio is 1.0599, with the average being 1.0660.

For FINO-1 at 60m the over prediction is greatest in neutral conditions and lowest in stable conditions. The max ratio is 1.0320 and min ratio is 1.0192 with the average ratio being 1.0262. At 80m the wind shear ratio is greatest in stable conditions and lowest slightly unstable conditions. Where max ratio is 1.1773 and min is 1.1567 with an average of 1.1652. The large gap between the values may be explained by the general lack of stability correction included in the method, where all correction is done in the power law exponent. The power law exponent is a fix constant as recommended in the GL standard (GL).

5.3.3 Logarithmic method with stability correction

The results of the velocity ratio of measured versus predicted and RMSE are presented in table 5.2-5.5, with roughness length varying as described in section 3.3. For FINO-3 at 70m the wind ratio shows that the method over-predicts the wind shear in all conditions except unstable, and that this over-prediction is similar for all stability conditions. There is a slight difference in the ratio depending on which roughness length that is used. The ratio is highest with z_0=0.01 and generally lowest with z_0=varying but z_0=0.01 give more or less the same results. When this method uses z_0=0.01 the highest ratio is in stable conditions with a ratio value of 1.050 and the lowest ratio is 0.995 in unstable conditions. For the profile using z_0=0.0001 the highest ratio is 1.028 and the min ratio is 0.989, with profile using z_0=varying highest ratio is 1.026 and lowest ratio is 0.989.

Wind speed ratio at 90m follows the same tendencies as that of 70m, with wind shear being over-predicted for all conditions. For the profile using z_0=0.01 the highest ratio is 1.110 and lowest ratio is 1.028. For the profile using z_0=0.0001 the highest ratio is 1.068 and the min ratio is 1.009, with profile using z_0=varying highest ratio is 1.027 and lowest ratio is 1.003.

For FINO-1 the wind shear at both heights are generally over predicted for all stability classes, with the exception of unstable conditions. Over-prediction is greatest in stable condition and lowest in unstable condition. At 60m the highest ratio when using z_0=0.01 is 1.0446 and the lowest ratio is 0.985. For the profile using z_0=0.01 the highest ratio is 1.045 and lowest ratio is 1.028. For the profile using z_0=0.0001 the highest ratio is 1.017 and the min ratio is 0.977, with profile using z_0=varying highest ratio is 1.018 and lowest ratio is 0.977.

For wind speeds at 80m the wind ratios are higher than that at 60m because of the larger height difference. As for 60m the highest ratio is given when using z_0=0.01, the ratio is largest in stable conditions having a value of 1.114 and lowest in unstable conditions where the ratio is 1.023. For the profile using z_0=0.0001 the highest ratio is 1.063 and the min ratio is 1.000, with profile using z_0=varying highest ratio is 1.064 and lowest ratio is 0.997.

5.3.4 Pena

The wind ratios from the Pena method (section 3.5) are presented in table 5.2-5.5. For FINO-3 at ratio 70m the results show that the wind shear is over predicted, and that ratio is greatest for stable conditions and likewise smallest for unstable conditions, the max ratio is 1.0212 and min is 0.9959. At 90m max ratio is 1.0521 and min ratio is 1.0016. Results from FINO-1 are generally the same as for FINO-3 with over-predictions being a slightly lower at this site. Wind shear is greatest in stable conditions and lowest in unstable conditions. At 60m max ratio is 1.0139 and min ratio is 0.9853, while for 80m max ratio is 1.0343 and min ratio is 0.9834.

5.3.5 RMSE

The RMSE values as defined in section 5.3 are presented in table 5.2-5.5 for the different methods. The RMSE results have been sorted using the stability criteria shown in table 5.1. After this filter had been used the data set contained 13108 (FINO-1) and 14888 (FINO-3) values respectively, this is equivalent to 24.7% (FINO-1) and 21.4% (FINO-3) of the original data set. The results of RMSE are relatively similar at both sites, with height 60m and 70m having lowest errors and opposite for 80m 90m. This is due to the height difference between the predicted wind speed and wind speed used to calculate the predicted wind speed is being lower for 60m and 70m than for 80m and 90m. For the logarithmic methods the error increases as the z_0 value increases, this is consistent expectations and with results presented earlier. The logarithmic method with stability correction got a higher error than the logarithmic without. This is unexpected since the method should improve the predicted wind shear, but can probably be explained by the stability correction over correcting in stable condition thereby increasing the error. Best RMSE results are shown by the Pena method, which constantly have one of the lowest errors and also good ratios.

6. Discussion

6.1 Comparison of results

In section 5 the results from the different methods in this thesis were presented, and both the figures, velocity ratio of measured and predicted and RMSE show that there are differences between the methods. A clear tendency is however seen in section 5 with results improving when corrections for stability and also ABL height are included. Especially the RMSE shows this improvement well. From table 5.2-5.5 RMSE results show that the Pena method allover have the best results. This is supported when comparing the wind ratios (table 5.2-5.5) and plots (figure 5.1-5.3).

6.2 Parameters used in the methods

To calculate wind speed is a difficult task because of the many aspects that influence it. In the theory section, which forms the basis for this thesis the most important parameters for calculating wind forces are explained. One of them is the roughness length and thereby also the friction velocity, which influence the wind speed within the SL. These parameters are important for calculating the wind speed. Calculation of these elements has been done using the Charnock relation. When applying this relation an actual wind speed has been required, and to obtain trustworthy results the wind recordings from the lowest vertical elevations has been used. For FINO-1 and FINO-3 this was at heights of 40m and 50m respectively. The effect of aerodynamic drag is largest closer to the ground, and it can be questioned whether the wind speeds at 40m and 50m are low enough to be affected sufficiently by this and thereby give good values for the roughness length. In the calculations the roughness length were found to be in the in the range of 1e-3 to 1e-5. Table 2.1 in DNV-RP-C205 gives an expected range of roughness length values, and it is to be between 1e-2 and 1e-4. When comparing ranges, the calculated values were found to be in the lower half of the expected range and below it.

An important basis in the presentation of the results in section 5 is the stability and therefore also the gradient Richardson number. The gradient Richardson number is calculated using eq. 2.4 in section 2.5. As described in this section the Ri_{grad} have a limitation when used to find the Monin-Obukhov length, where all values above 0.2 are invalid. A similar limitation is not used for negative values, and large negative values for Ri_{grad} are therefore not excluded. This have resulted in unlikely large results of gradient Richardson number being used in calculations, which have lead to unreasonable values of L_{MO} boundary layer height and also the stability parameter. The gradient Richardson number requires stationary conditions to be used and the filter applied in the calculation may not be sufficient. Also the Ri_{grad} uses temperature measured at the site, and errors in these measurements will give wrong values of Ri_{grad}.

In the methods with stability correction the stability parameter is an essential element. As of now no standard stability parameter is given, instead different standard (DNV) and publication (Holtslag) suggest different methods. It is therefore difficult to conclude on the values related to the stability correction. In general the values of correction seem high with an average range of 5-8 [ms^{-1}], while an expected range would be 2 ms^{-1} and lower. This is closely related to the values of Monin-Obukhov length that is used in the stability correction function.

6.3 Results compared to other publications

Offshore wind profiles have been investigated in several other studies and standards, where stability corrections are estimated using different methods (DNV, Tambke. 2005, Barthelmie. 2010 and Pena. 2011) depending on what have been studied. Among these studies there are some that are more relevant to this study because of the methods that are applied. Particularly Tambke et al.2005, Barthelmie et al.2010 and Pena et al.2011, which are methods investigated in this thesis. Also the master thesis by Venora et al.2009, where stability corrections are investigated using among other the gradient Richardson number.

In figure 4.2 from Venora's thesis wind speeds difference between 33m and 50m in FINO-1 and 21m and 70m in Egmond aan Zee are used to estimate the wind speed at 90m and 116m respectively (Venora 2009). In figure 4.2 (Venora 2009) plots of wind profiles using the gradient Richardson number are presented applying data from FINO-1 (left graphs) and Egmond aan Zee (right graphs). The upper left graph shows the wind speed ratio at two heights, in the graph plots using the power law, logarithmic and logarithmic MOST method are shown. When this figure is compared with figure 5.2 and 5.4 the plots corresponds well with each other and follow the same tendencies in the ratio. This can be interpreted to indicate that the method is applied correctly and strengthens the credibility of the results using power law, logarithmic and logarithmic with stability corrections methods.

In the paper published by Pena et al.(2011) it is concluded that logarithmic with stability corrections profiles provide a good prediction for unstable and neutral conditions but over-predicts when coming in to stable conditions. When applying an added correction term involving the ABL height the over-prediction in stable conditions is reduced, and results fit well with observations. These outcomes agree well with results presented in table 5.1-5.4 and figure 5.3-5.6.

The wind ratios and RMSE presented in table 5.1-5.4 describe the relationship between the estimated and measured wind, and also the error of the obtained results. The values associated with these result are important because they describe how accurate the estimated wind speeds are. In the paper published by Barthelmie et al (2010) they presented similar results, where ratio and RMSE results from

among other the logarithmic, logarithmic with stability corrections and Pena methods. The results in Barthelmie et al.(2010) showed that ratios in stable and slightly stable conditions were under-predicted, while in slightly stable and stable conditions wind shear was over-predicted or slightly under-predicted. This is different than results presented in section 5.3, where tables 5.2-5.5 show that wind shear generally is over-predicted in stable and slightly-stable conditions. The differences in wind speed ratios might be explained by site variations as wind speed, fetch length or distance from cost. Also in Barthelmie et al (2010) wind speeds were calculated from wind speed at 10m. This gives a larger height difference between the predicted wind speed and the wind speed that is used to calculate it, which could explain why the RMSE are higher. The RMSE in Barthelmie are higher than those in table 5.2-5.5, which may also explain some of the difference. The low values of RMSE in tab. 5.2-5.5 indicate that the calculation of wind speed are done correct and that they are reliable.

7. Conclusion

In pursuit of more stable and cleaner energy resources wind turbines are being placed both further offshore and in greater heights. This has increased the need for better understanding of the wind profiles over water. In this thesis different methods of calculating wind profiles have been investigated and compared. The methods consist of the recommended method from DNV (logarithmic) and GL (power law) and also suggested methods published by Barthelmie, Pena and Tambke. The methods have been calculated using wind speed recordings from FINO-1 and FINO-3 and then extrapolated for higher vertical elevations. These calculated wind speeds have then been plotted and compared to the measured wind speeds at certain heights (60m & 80m for FINO-1, and 70m & 90m for FINO-3).

Results are presented in the form of figures (5.1-5.4) showing the plot of predicted and measured wind speed ratio between to heights, and also tables (5.2-5.5) containing the wind speed ratio between predicted and measured and the RMSE. When analyzing the results it is clear that the Pena method gave the most accurate results. With the predicted ratio plot giving best correction compared to the measured plot, and also RMSE being low (rang between 0.31-0.83 depending on which height and site is studied). The other methods also gave reasonable results, but either lacked stability correction in the method or over-corrected in stable condition. Results also showed that roughness length had a big impact on the wind speed, and that it is important to calculate the roughness length and not just assume a value. In this thesis it was meant to investigate the Barthelmie and Tambke methods also. This was not possible to do because of lack of high resolution recordings for the Barthelmie method, and problems with recreating the method as described in the paper for the Tambke method. A possible solution for the Tambke method may have been found (described in subsection 5.2.4), but due to time constraints this was not investigated.

The result presented in this thesis show that the present attempt by the standards to compensate for the increased wind speed in stable conditions, have shown to be too conservative. Further research and implementation of stability corrections in stable conditions should be done, so that over prediction of wind shear in the stable condition is reduced.

As part of this further work it is recommended to investigate the two methods that were not examined in this thesis. Especially the Barthelmie method is interesting because of the possibility to include ABL height correction. It would also be interesting to calculate the methods using Bulk Richardson number and to compare the results with that of gradient Richardson number. This has been bone by Venora et al. 2009, but only for the power law and logarithmic profile with and without stability correction. It is also a need to get a standard method for classifying stability classes. At present several suggestions are available for both gradient Richardson number and Monin-Obukhov, but these vary in both number of stability classes and the range of the classes.

8. References

- Barthelmie, R. J., Sempreviva, A. M. and Pryor, S. C. The influence of humidity fluxes on offshore wind speed profiles. 2010.
- Businger, J., Wyengaard, J., Izumi, Y. and Bradly, E., 1971: Flux-profile relationship in the atmospheric surface layer.
- Bye, J. A. T. Inertially coupled Ekman layers. 2001
- DNV-RP-C205(2010) "Environmental Conditions & Environmental Loads " October.
- Eugster, A. Onshore lidar wind profile measurements at Utsira and their benefit for offshore wind turbine design and operation. 2010.
- Germansher Lloyds (2005) "Guidelines for the Certification of Offshore Wind Turbines" Ed 2005.
- Glickman, Todd S. *Glossary of Meteorology* (2nd ed.). American Meteorological Society, 2000
- Grachev, A., Fairall, C. and Bradley, E., 2000: Convective profile constraints revisited. Boundary layer Meteorol., 94, 495-515.
- Gryning, S. E., Batchvarova, E., Brümmer, B., Jørgensen, H., Larsen, S. On the extention of wind profile over homogeneous terrain beyond the surface boundary layer. 2007.
- Holtslag, A. A. M. Estimate of diabetic wind speed profiles from near-surface weather observations. 1984.
- Obhrai, C., Kalvig, S., Gudmestad, O.T., A review of current guidelines to determin wind design parameters for offshore wind turbines. 2011.
- Obhrai, C. Improved Design Criteria and Forcast for Energy Yield fomr Offshore Wind Turbines. 2011.
- Obukhov, A.S. TURBULENCE IN AN ATMOSPHERE WITH A NON-UNIFORM TEMPERATURE. 1971.
- Sathe, A., S.E. Gryning, S.E. and Pe˜na, A. Comparison of the atmospheric stability and wind profiles at two wind farm sites over a long marine fetch in the North Sea. *Wind Energy*, 2011
- Stull, R. B.: An introduction to boundary layer metrology, Kluwer Publication Ltd, Dordrecht 1988.
- Tambke, J., Lange, M., Focken, U., Wolff, J., and Bye, J.: Forecasting offshore wind speeds above the North Sea, Wind Energy, 8, 3-16, 2005
- Tambke, J., Claveri, L., Bye, L., Poppinga, C., Lange, B., von Bremen, L., Durante, F., Wolff, J., Offshore Meteorology for Multi-Mega-Watt Turbines, *Proceedings EWEC 2006*.
- Toba Y. Local balance in the air-sea boundary process III. On the spectrum of wind waves. J. Oceanor. Soc. Of Japan, 29: 209-220, 1973.
- Turner, J.S. Buoyancy Effects in Fluids. Cambridge University Press, 1979.
- Venora, A.: Monin-Obukhov Similarity Theory Applied to Offshore Wind Data. 2009.
- Woods, J.D. : On Richardson's number as a criterion for laminar-turbulent-laminar transition in the ocean and atmosphere. *Radio Science*, 4(12):1289–1298, 1969.

9. Appendix

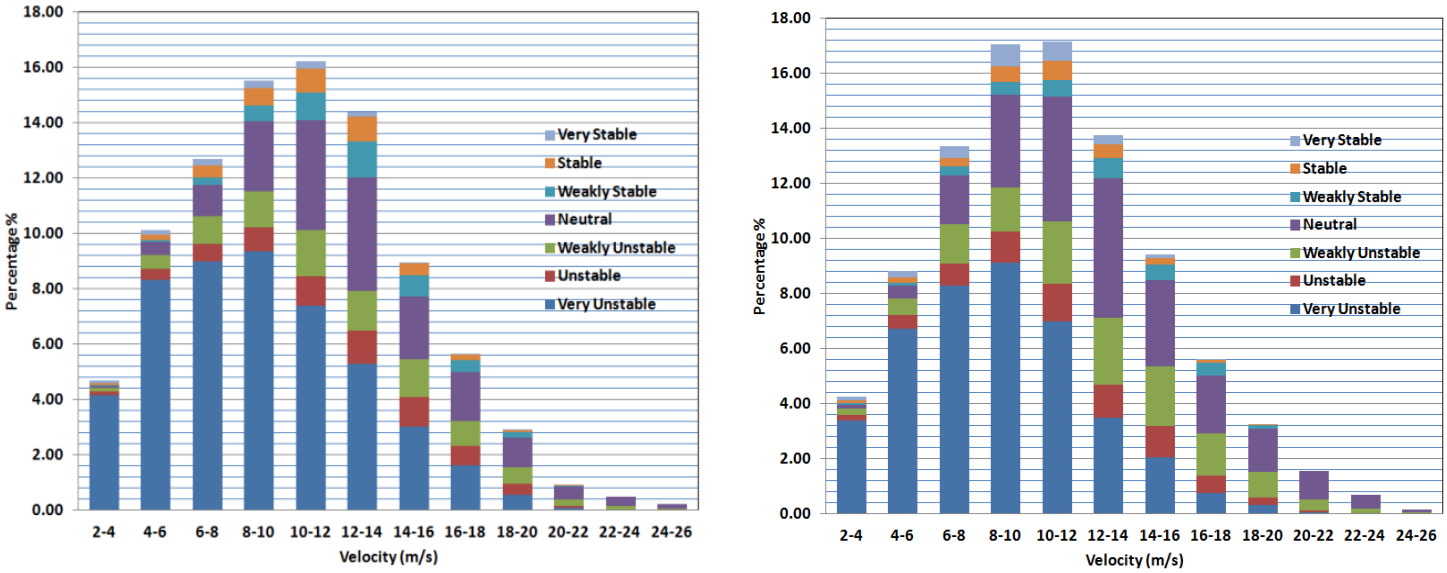

Figure 9-1: Distribution of wind speed at FINO-3 and FINO-1 for each stability class

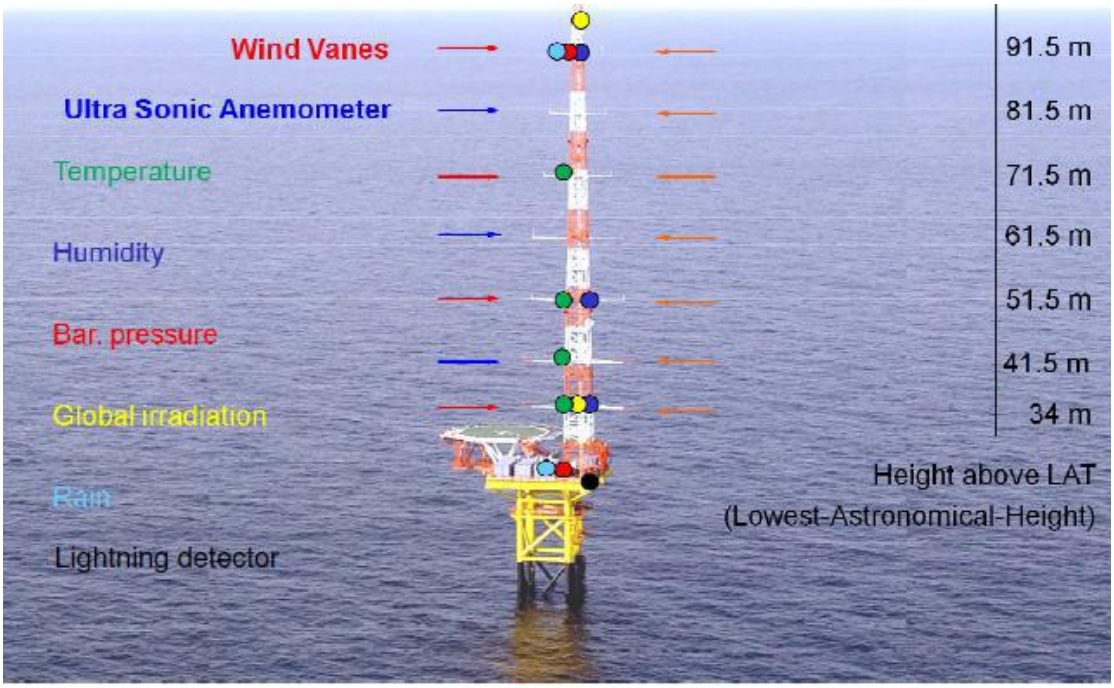

Figure 9-2: picture of FINO-1 showing the placement of measurement equipment (Obhrai 2012).

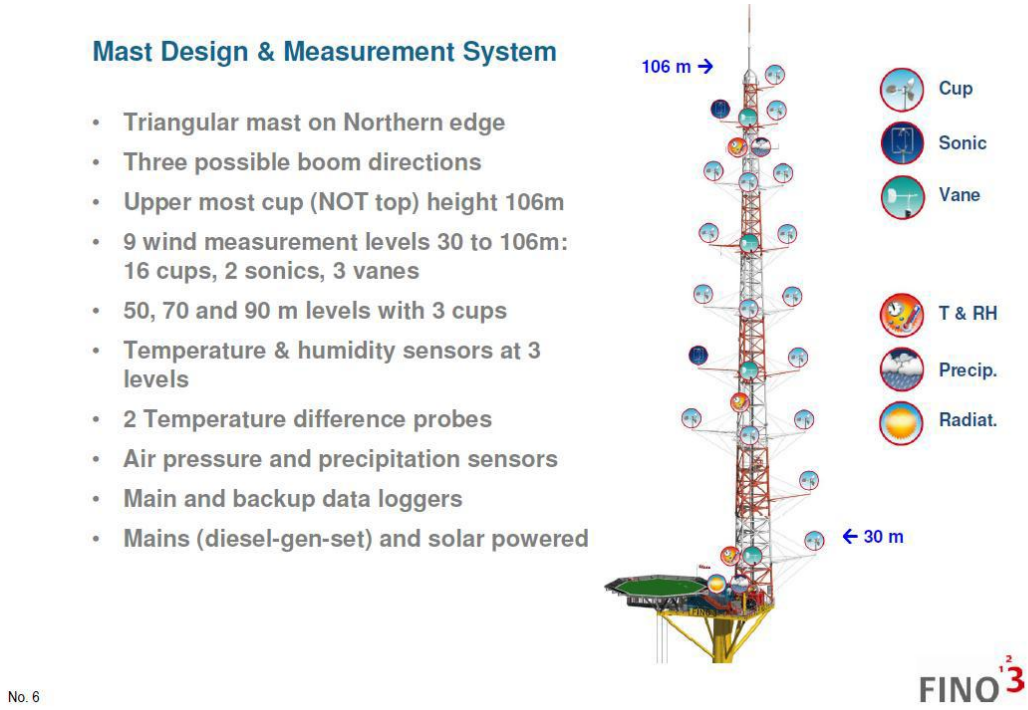

Figure 9-3: Model of FINO-3 describing mast design, measurement system and placement. (Obhrai 2012)

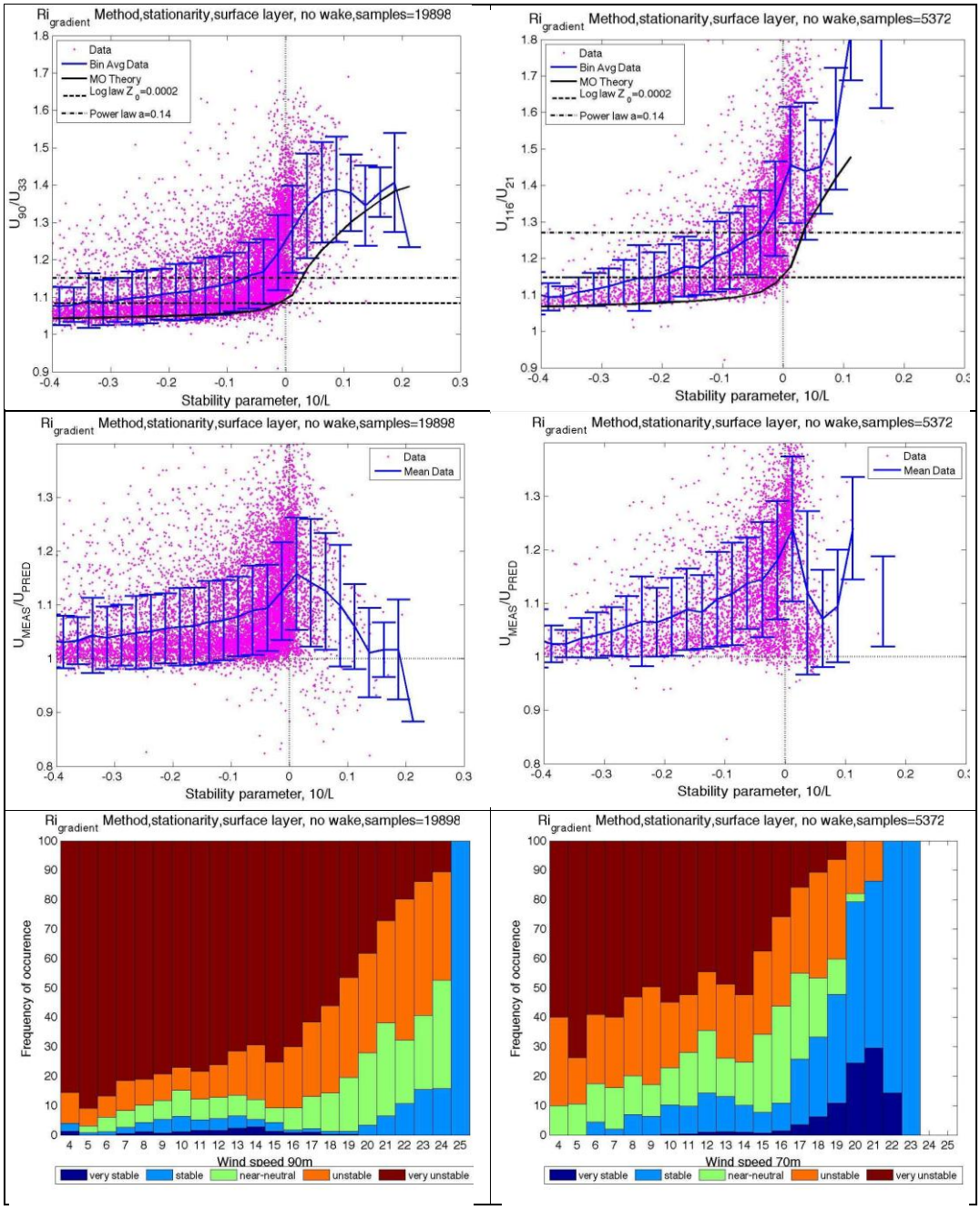

Figure 4.2: Richardson Gradient Method results for FINO-1 (left graphs) and Egmond aan Zee (right graphs). Wind speed ratio at 2 levels (top graphs), measured and predicted wind speed ratio at 90m in FINO-1 and 116m in Egmond aan Zee (middle graphs) and frequency of stratification occurrence (bottom graphs). The error bars represent the standard deviation of the data. The results are reported using stationary and surface layer filters.

Figure 9-4: Results from Venora 2009